THE GEOLOGICAL SOCIETY
OF AMERICA®

Time-progressive mantle-melt evolution and magma production in a Tethyan marginal sea: A case study of the Albanide-Hellenide ophiolites

Emilio Saccani[1],*, Yildirim Dilek[2],*, and Adonis Photiades[3],*
[1]DIPARTIMENTO DI FISICA E SCIENZE DELLA TERRA, UNIVERSITÀ DI FERRARA, VIA SARAGAT 1, 44100 FERRARA, ITALY
[2]DEPARTMENT OF GEOLOGY AND ENVIRONMENTAL EARTH SCIENCE, MIAMI UNIVERSITY, 118 SHIDELER HALL, 250 S. PATTERSON AVENUE, OXFORD, OHIO 45056, USA
[3]DEPARTMENT OF GENERAL GEOLOGY AND GEOLOGICAL MAPPING, INSTITUTE OF GEOLOGY AND MINERAL EXPLORATION (IGME), OLYMPIC VILLAGE, 13677 ACHARNAE, ATTICA, GREECE

ABSTRACT

We present a comprehensive overview of the melt evolution of the upper mantle peridotites and different lava types occurring in the Jurassic Albanide-Hellenide ophiolites, based on new and extant geochemical data and trace element modeling. Peridotites consist of lherzolites and harzburgites that are variably depleted, and show increasing light rare earth element (LREE) enrichment with increasing whole-rock depletion. The spatial-temporal relationships of volcanic rocks indicate four discrete types with progressively younging ages: (1) normal mid-oceanic ridge basalts (N-MORBs); (2) medium-Ti basalts (MTBs); (3) island arc tholeiitic (IAT) basalts; (4) boninitic rocks. Our REE modeling reveals the following results. (1) Moderately depleted lherzolites represent N-MORB mantle residua produced by 10%–20% partial melting of a depleted MORB mantle source. Melt extraction formed N-MORB lavas. (2) Residual lherzolite underwent 5%–8% partial melting without any subduction influence, producing MTB magmas. (3) Following subduction initiation, these refractory lherzolites were enriched in LREEs by subduction-derived fluids. Their partial melting (~10%–20%) generated IAT magmas. (4) With continued subduction, the highly depleted residual mantle left after the previous melting events underwent significant LREE enrichment and high degree (15%–25%) partial melting, producing the youngest, boninitic rocks. The residual mantle after boninitic melt extraction is represented by extremely refractory harzburgites. This progressive melt evolution of the upper mantle peridotites and volcanic rock types is compatible with that of the subduction initiation–related magmatism and mantle dynamics in the Izu-Bonin-Mariana arc-trench rollback system, and indicates a time-progressive mantle-melt evolution in the upper plate of the Tethyan subduction system.

INTRODUCTION

Regional Ophiolite Perspectives

The Dinaride-Albanide-Hellenide mountain system is characterized by the occurrence of two north-northwest–south-southeast–trending parallel belts of Tethyan ophiolites and ophiolitic mélanges. These Tethyan paleo-oceanic domains include the Vardar zone of the Eastern Hellenides in the east, and the Mirdita and Subpelagonian-Pelagonian zones of the Albanides and Western Hellenides (respectively) in the west (Fig. 1; Dilek et al., 2005, 2007, 2008; Saccani et al., 2011; Ferrière et al., 2012).

The Mirdita and Subpelagonian-Pelagonian oceanic domains include Middle Jurassic ophiolites displaying both mid-ocean ridge and suprasubduction zone (SSZ) affinities. The earlier studies on the Mirdita ophiolites in the north-central section of the Albanides, as well as in its southern continuation in the Pindos-Vourinos segment of the Western Hellenides, led to the recognition of Tethyan oceanic lithosphere sequences with distinctly different lithological units, petrology, and geochemistry (e.g., Dede et al., 1966; Capedri et al., 1982; Beccaluva et al., 1984, 1994; Shallo et al., 1987; Jones and Robertson, 1991; Smith, 1993; Shallo, 1994; Shallo and Dilek, 2003; Saccani et al., 2004). Relatively thin (3–4 km) and commonly incomplete ophiolite sequences (for an updated definition of an ideal ophiolite sequence, see Dilek and Furnes, 2011, 2014) displaying mid-oceanic ridge basalt (MORB) geochemical affinities were recognized in the west, whereas thicker (10–12 km), complete ophiolite sequences showing SSZ affinities were recognized in the east within the same ophiolite belt. Various interpretations have been suggested for this geochemical dualism (for a detailed discussion, see Dilek et al., 2008), which has been taken as a result of distinctly different timing and tectonic settings of their formation. The MORB lithosphere currently exposed in the west formed during a seafloor-spreading phase in a Tethyan marginal basin, whereas the SSZ lithosphere in the east developed following the initiation and establishment of an intraoceanic subduction zone within the same basin (e.g., Dede et al., 1966; Shallo, 1992; Beccaluva et al., 1994; Bortolotti et al., 2005).

Outstanding Problems

Recent studies of the Tethyan ophiolites in the Albanide-Hellenide mountain belt and their findings have shown, however, that this twofold subdivision is not as sharp, spatially and temporally, as previously thought.

Emilio Saccani ⓘ http://orcid.org/0000-0001-9879-2795
*Emails: Saccani: sac@unife.it; Dilek: dileky@miamioh.edu; Photiades: fotiadis@igme.gr.
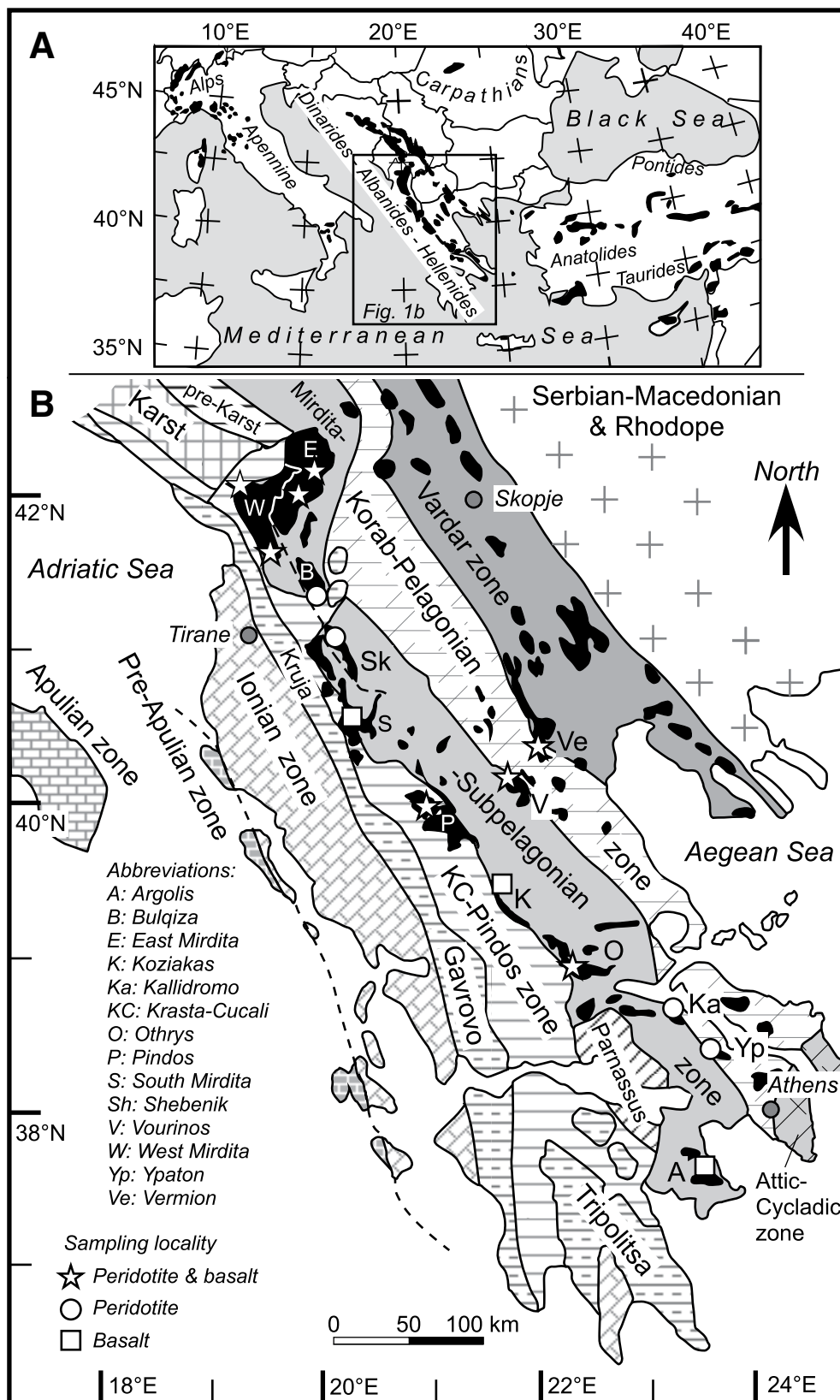
Figure 1. (A) Distribution of the main ophiolite massifs in the Mediterranean region and the location of the study area. (B) Simplified tectonic map of the Albanide-Hellenide orogenic belt showing the main tectonostratigraphic zones and ophiolite massifs. Compiled after Dilek et al. (2007, 2008), and Bortolotti et al. (2013).

The extrusive sequences of the Western Mirdita (WMO) and Pindos ophiolites include volcanic rocks with SSZ affinities that are interlayered with typical MORB lavas, are crosscut by boninitic dikes, and are overlain by boninitic lava flows (Jones and Robertson, 1991; Bortolotti et al., 1996, 2002; Bébien et al., 2000; Saccani and Photiades 2004; Dilek et al., 2005). Similarly, typical MOR-type intrusive rocks in the Eastern Mirdita ophiolite (EMO) within the south-central Albanides exhibit mutual crosscutting relationships with those having SSZ geochemical signatures (Manika et al., 1997; Bébien et al., 1998; Koller et al., 2006). The ophiolites in the southern Albanides, Pindos (Dramala Complex), Koziakas, Othrys, and Vermion contain both lherzolitic (i.e., MORB type) and harzburgitic (i.e., SSZ type) mantle tectonites (Hoeck et al., 2002; Photiades et al., 2003; Saccani et al., 2003; Saccani and Photiades, 2004; Barth et al., 2008). These observations collectively indicate that both the WMO and EMO underwent complex petrogenetic evolution of different magma types, which partially coexisted in both time and space.

Field-based systematic geochemical studies have demonstrated that the WMO and EMO in the Albanides and the Pindos ophiolites in the Western Hellenides developed through a time-progressive evolution of magmas from normal-type (N) MORB to medium-Ti basalt (MTB), island arc tholeiite (IAT), and boninite in an SSZ setting that underwent rapid slab rollback (Dilek et al., 2008; Dilek and Furnes, 2009; Saccani et al., 2011). A corollary to this finding is that the apparent geochemical dualism (i.e., MORB versus SSZ affinities) observed in the Albanide-Hellenide ophiolites does not require either separate tectonic settings or significantly different times of formation (Dilek et al., 2008; Saccani et al., 2011). A similar geochemical evolution has been observed in the Izu-Bonin-Mariana (IBM) forearc lithosphere (Van der Laan et al., 1992; Pearce et al., 1992; Bloomer et al., 1995; Stern et al., 2003), as well as in the Troodos-Cyprus (see Dilek and Furnes, 2009), Kizildag-Turkey (see Dilek and Thy, 1998, 2009), and Kudi–northwest China (Yuan et al., 2005), and other SSZ ophiolites around the world (see Dilek and Newcomb, 2003; Dilek, 2003; Dilek and Robinson, 2003).

These conclusions were reached largely based on a careful delineation of the internal structure and architecture of the ophiolites, as well as on systematic geochemistry and chemostratigraphy (i.e., chemical variations across volcanic rock units in a well-defined stratigraphy of an extrusive sequence) of volcanic rocks and dikes. However, it is commonly accepted that the compositional differences between magma types in ophiolites are related to different mantle source characteristics and/ or partial melting degrees (e.g., Pearce, 1982). The mantle tectonites in the Albanide-Hellenide ophiolites show a wide compositional spectrum, ranging from lherzolites and clinopyroxene (cpx) poor lherzolites to cpx-bearing harzburgites and cpx-free harzburgites. However, the geochemistry and the petrological significance of these mantle peridotites have not been well documented, and so their melt evolution through time and space is relatively unknown.

Objectives of This Paper

In this paper we present a systematic field-based geochemical study of the upper mantle peridotites in the Jurassic Tethyan ophiolites in the Albanides-Hellenides and discuss their progressive petrogenetic evolution in both time and space. The main focus of this study is to define the characteristics of different peridotite types and associated magmatic units in the ophiolites, and then to examine the melt-mantle residua relationships as recorded in the whole-rock major and trace element geochemistry and in the rock textures of the peridotites. We first present our new and published geochemical data, as well as some of the data in the literature to characterize the ophiolitic peridotites and different magma types, as represented by geochemically distinct extrusive rock units. We then introduce our rare earth element (REE) modeling method and results to define the melt, mantle residua and melt-mantle source relationships for each identified magma type within the ophiolites. We use our modeling results, combined with field-based geochemistry (i.e., observing and documenting geochemical variations within a stratigraphically and structurally well constrained volcanic sequence), to develop a petrogenetic-geodynamic model to explain the progressive evolution through time and space of the peridotites and different magma types in the Albanide-Hellenide ophiolites. Our model provides an ideal case study to probe in four dimensions the chemical geodynamic evolution of the oceanic upper mantle both in ancient and modern SSZ tectonic environments.

REGIONAL GEOLOGY AND TECTONIC ARCHITECTURE OF THE ALBANIDE-HELLENIDE OPHIOLITES

The Dinaride-Albanide-Hellenide belt (Fig. 1A) is part of the Alpine orogenic system, which formed as a result of the diachronous collision of Adria with Eurasia in the Cenozoic (Dilek, 2006). The south-central segment of this belt (i.e., from Albania to Greece) consists of a series of tectonic domains, which include, from west to east: (1) the rifted continental margin of Adria, composed of a west-vergent imbricate stack of five tectonostratigraphic zones; (2) the Mirdita-Subpelagonian Tethyan ophiolitic zone; (3) the Korabi-Pelagonian zone, consisting of crystalline basement units with Gondwana affinities; (4) the Vardar ophiolitic zone; and (5) the Serbian-Macedonian and Rhodope continental blocks with Eurasia affinities (Fig. 1B).

The Jurassic ophiolites crop out extensively in both the Mirdita-Subpelagonian and Vardar zones, and as tectonic klippen or erosional remnants in the Korabi-Pelagonian zone (Fig. 1B). Both the Mirdita-Subpelagonian and the Korabi-Pelagonian ophiolites are tectonically underlain by a subophiolitic mélange unit (i.e., the Rubik Complex of Bortolotti et al., 2013). Thrust slices of granulite to amphibolite and greenschist facies metapelitic and metamafic rocks occur discontinuously between the ophiolitic peridotites above and the mélange below. Radiolarian cherts intercalated with and overlying the volcanic sequences in the WMO and EMO in the Albanides have revealed Bathonian to early Callovian and Bathonian to late Oxfordian ages, respectively (Marcucci and Prela, 1996; Chiari et al., 2002, 2004). However, the sedimentary cover of the Vourinos volcanic sequence in the Hellenides is latest Bajocian in age (Chiari et al., 2003).

The extrusive sequences in the ophiolites display both MORB and SSZ affinities (Beccaluva et al., 1994; Shallo, 1994; Bébien et al., 2000; Dilek et al., 2008). Generally, the MOR-type sequences occur in the western part of this zone (e.g., West Mirdita, Pindos), whereas the SSZ-type sequences are largely exposed in the eastern part (e.g., East Mirdita, Vourinos; Rassios and Dilek, 2009), as well as in the Korabi-Pelagonian zone to the east (e.g., Vermion ophiolites; Saccani et al., 2008a).

Although mainly composed of MORB-type rocks, the extrusive and intrusive rock sequences in the WMO and Pindos ophiolites also include significant volumes of SSZ rocks. The EMO to the east contains only minor volumes of typical MOR-type plutonic rocks (e.g., Bortolotti et al., 1996, 2002; Manika et al., 1997; Bébien et al., 1998, 2000; Insergueix-Filippi et al., 2000; Hoeck et al., 2002; Koller et al., 2006; Barth et al., 2008; Barth and Gluhak, 2009; Saccani et al., 2011). Figure 2 shows generalized columnar sections of different ophiolite occurrences in the Albanide-Hellenide belt.

A typical ophiolite sequence in the WMO includes, from bottom to top (Fig. 2A), (1) lherzolitic mantle tectonites; (2) a layered mafic-ultramafic cumulate succession; (3) a mafic to differentiated intrusive complex; (4) a poorly developed sheeted dike complex; and (5) an extrusive sequence.
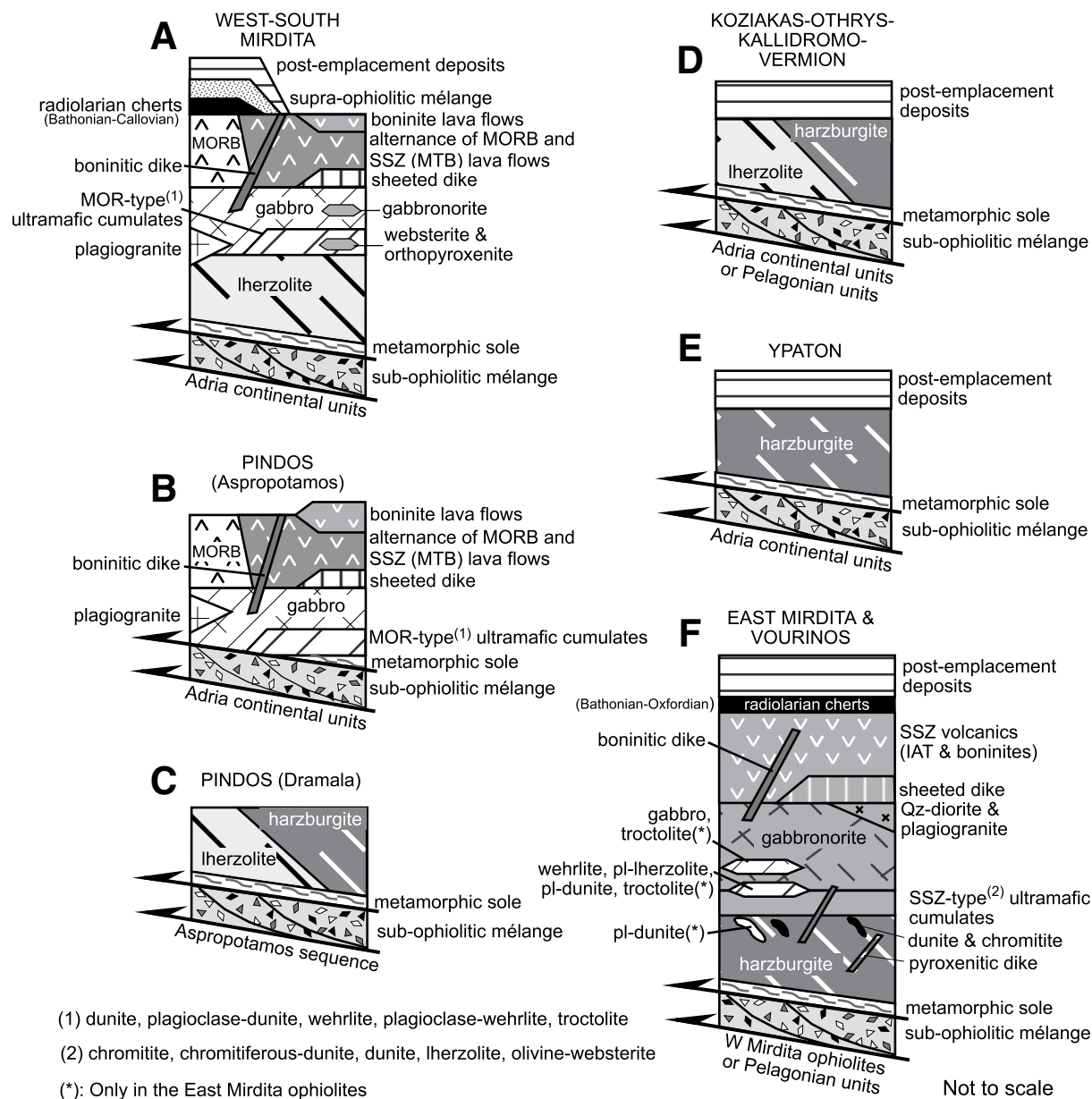
Figure 2. Reconstructed stratigraphic columnar sections of the main ophiolite massifs in the Albanide-Hellenide ophiolites. Modified from Saccani et al. (2011, and references therein). MOR—mid-ocean ridge; MORB—mid-oceanic ridge basalt; SSZ—suprasubduction zone; MTB—medium-Ti basalt; IAT—island arc tholeiite; Qz—quartz; pl—plagioclase.

The intrusive complex mainly comprises typical MORB-type rocks, composed of dunites, plagioclase dunites, troctolites, wehrlites, melagabbros, and gabbros, as well as rare Fe gabbros, plagiogranites, and gabbronorites. It also includes websterites, orthopyroxenites, and gabbronorites with characteristic SSZ geochemical fingerprints, especially in the southern Albanides (Hoeck et al., 2002; Koller et al., 2006). The extrusive sequence contains basaltic pillow lavas with N-MORB affinity, as well as some volcanic successions in which N-MORBs alternate with MTBs. These mixed volcanic series are crosscut by boninitic dikes and locally topped by boninitic lava flows (Bortolotti et al., 1996, 2002; Bébien et al., 2000; Hoeck et al., 2002; Saccani et al., 2011).

The crustal units (i.e., Aspropotamos sequence) of the Pindos ophiolite in the Western Hellenides are compositionally similar to that of the WMO in the Albanides to the north (Fig. 2B). However, the structural order in the Pindos ophiolite is inverted such that the upper mantle series (i.e., Dramala Complex; Fig. 2C) tectonically overlies the crustal units; the Dramala Complex includes both lherzolites and harzburgites (Jones and Robertson, 1991; Saccani and Photiades, 2004). The Koziakas, Othrys, Kallidromon, and Vermion ophiolites (Fig. 2D) consist of incomplete ophiolite massifs with mantle tectonites made of both lherzolites and harzburgites; the Ypaton ophiolite (Fig. 2E) includes only harzburgites (Capedri et al., 1985; Saccani et al., 2003, 2008a).

A reconstructed igneous stratigraphy of the EMO and Vourinos ophiolites (Fig. 2F) includes (from bottom to top): (1) mantle tectonites represented by depleted harzburgites; (2) a layered mafic-ultramafic cumulate succession; (3) a mafic to differentiated intrusive complex; (4) a thick

sheeted dike complex; and (5) an extrusive sequence. The upper part of the harzburgites locally contains dunite and chromitite pods and lenses, the abundance of which increases toward the top of the mantle section showing a transition to the overlying cumulates. Ultramafic cumulates consist of dunites with chromitite layers, olivine-websterites, and websterites. Both cumulate and isotropic plutonic rocks at the bottom are largely olivine-gabbronorites and gabbronorites, which are replaced upward by abundant quartz diorite and plagiogranite rocks. The sheeted dike complex and the extrusive sequence include rocks with compositions of basalts, basaltic andesites, andesites, dacites, and rhyolites, showing both IAT (low Ti) and boninitic (very low Ti) affinities (Beccaluva et al., 1984, 1994; Shallo, 1994; Bortolotti et al., 1996; Bébien et al., 2000; Dilek et al., 2007, 2008; Saccani et al., 2008b; Phillips-Lander and Dilek, 2009). Extrusive rocks occur as both massive and pillow lavas. The entire ophiolite complex is locally crosscut by boninitic dikes. The EMO and Vourinos ophiolites are largely represented by typical SSZ-type ophiolitic rocks. However, in the south-central Albanides the ophiolite massifs include plagioclase lherzolites and troctolites locally occurring in the cumulate successions, and troctolites and gabbros within gabbronoritic series (e.g., Bortolotti et al., 1996, 2002; Manika et al., 1997; Bébien et al., 1998, 2000; Insergueix-Filippi et al., 2000; Hoeck et al., 2002; Koller et al., 2006; Barth et al., 2008; Phillips-Lander and Dilek, 2009; Barth and Gluhak, 2009; Saccani et al., 2011).

DATABASE AND CONSTRAINTS ON SAMPLE SELECTION

We have evaluated and used in this study a total of 97 samples of upper mantle peridotites and 47 samples of Jurassic basaltic rocks representing different magmatic affinities. Only relatively primitive basaltic rocks (i.e., MgO > 7% on anhydrous bases) were selected because they can reasonably be assumed to represent liquid compositions of different magma types, similar to primitive liquids generated from mantle partial melting. We have used in this study new and previously published data. In detail, we have analyzed during the course of this study 46 new samples of upper mantle peridotites from the northern Mirdita, Bulqiza, and Shebenik massifs in Albania, and from the Pindos, Othrys, Ypaton, and Kallidromon massifs in Greece (see GSA Data Repository Table DR1[1]). Literature-based data are largely represented by samples that we collected. The use of these data allows an accurate selection of the most representative samples based on well-constrained geological, biochronological, petrographic, and analytical information. These data include 29 samples of upper mantle peridotites and 41 samples of basaltic rocks from various localities. However, in order to have a full coverage of different ophiolite massifs in the Albanides-Hellenides, we have also used some other existing data in the literature including 22 samples of mantle peridotites from the Othrys massif (Barth et al., 2008) and 6 basaltic samples from the WMO and Othrys (Hoeck et al., 2002; Monjoie et al., 2008). Detailed references for literature-based data are given in Tables DR2 and DR3. The regional distribution of the new and literature-based data is shown in Tables DR1–DR3, as well as in Figure 1B.

MINERAL ASSEMBLAGES AND TEXTURES

The petrographic study was carried out on both new peridotites presented herein and literature-based peridotites that we collected. All of them have spinel facies mantle mineral assemblages, consisting of olivine (ol),

orthopyroxene (opx) ± cpx as the main mineral phases and chromian spinel (Cr-spl) as an accessory phase. The modal amount of cpx is highly variable, ranging from 14% in the most fertile samples to 0% in the most depleted samples. Based on the modal composition, mantle peridotites are subdivided into: (1) lherzolites, (2) cpx-poor lherzolites, and (3) harzburgites.

In describing and characterizing the upper mantle peridotites investigated in this study, we follow the textural classification scheme of Mercier and Nicolas (1975). The lherzolites and cpx-poor lherzolites commonly display porphyroclastic textures, in which porphyroclasts are generally represented by both opx and cpx, and rarely by ol. Porphyroclasts commonly consist of large (5–7 mm), strained and elongated grains surrounded by small (0.5–1 mm) polygonal crystals mostly represented by ol. Kink-bands in ol and opx are common. Both cpx and opx porphyroclasts generally show mutual exsolution lamellae, whereas small, recrystallized grains (polygonal neoblasts) are generally free from exsolutions. Cr-spl shows xenomorphic shapes and commonly occurs as reddish to light brown fine-grained (0.5–1 mm) crystals in lherzolites, whereas in cpx-poor lherzolites it generally forms brown, medium-grained (1–2 mm) crystals. The modal composition of each sample is given in Tables DR1 and DR2. In summary, lherzolitic rocks consist of ol (65%–72%), opx (15%–24%), cpx (9%–14%), and Cr-spl (0%–3%), whereas cpx-poor lherzolites consist of ol (70%–72%), opx (21%–23%), cpx (5%–7%), and Cr-spl (0%–1%).

Harzburgites mostly show porphyroclastic textures with coarse-sized (5–10 mm) opx porphyroclasts and small (0.5–1 mm) neoblasts mainly consisting of ol. Locally, ol porphyroclasts can also be observed. Generally, porphyroclasts form strained and elongated grains. Very few samples show equigranular texture with grain size of ~2 mm. Ol is characterized by kink bands, and opx contains cpx exsolution lamellae. Cr-spl is scattered in the rocks and occurs either as xenomorphic or subhedral crystals with variable sizes (from ~0.3 to ~2 mm), and generally shows dark brown to black colors. However, in a few samples, Cr-spl shows idiomorphic shapes. Several samples display ~2–3-mm-scale lineations. Diopsidic cpx composes <2%–3% of many samples, although some samples are totally free of cpx. Harzburgites generally consist of ol (68%–79%), opx (18%–30%), cpx (0%–4%), and Cr-spl (0%–5%) (for the detailed modal composition, see Tables DR1 and DR2). We have paid particular attention in selecting the least altered samples for our analyses. Most samples show a degree of serpentinization ranging from 10% to 20%. However, a limited number of samples show the effects of moderate to advanced serpentinization (to 50%–60%). These samples are all harzburgites from the Skanderbeu (central Mirdita) and Vermion (Hellenides) ophiolites. Alteration minerals include serpentine, chlorite, and talc, as well as minor Fe-Ti oxides. Upper mantle peridotites from the Othrys massif described by Barth et al. (2003) display mineral assemblages and textures very similar to those outlined above. However, some of them contain significant volumes of modal plagioclase (pl). These plagioclase peridotites contain generally concordant millimeter-scale lenses of pl ± cpx ± opx, which were interpreted as a result of refertilization of previously depleted tectonites by an impregnating melt (Barth et al., 2003).

ANALYTICAL METHODS

The new samples of upper mantle peridotites presented in this paper were analyzed at the Dipartimento di Fisica e Science della Terra, Università di Ferrara (Italy). Whole-rock major and trace element (Zn, Cu, Sc, Ga, Ni, Co, Cr, V, Rb, Ba, Sr, Zr, and Y) compositions were determined by X-ray fluorescence (XRF) on pressed-powder pellets, using an ARL Advant-XP automated X-ray spectrometer. The matrix correction method proposed by Lachance and Trail (1966) was applied. Volatile contents were determined as loss on ignition (LOI) at 1000 °C. In addition, Rb, Sr, Y, Zr, Nb, Hf, Ta,

Th, U, and REEs were determined by inductively coupled plasma–mass spectrometry (ICP-MS) using a Thermo Series X-I spectrometer. Accuracy and detection limits for both XRF and ICP-MS analyses were determined using several international reference standards, as well as internal standards run as unknowns. Whole-rock compositions are given in Table DR1, and the accuracy and detection limits are reported in Table DR4.

## GEOCHEMICAL CHARACTERIZATION OF PERIDOTITES AND LAVAS

Upper Mantle Peridotites

The lack of any correlation between the contents of MgO, Ni, CaO, and Al_2O_3 and the LOI values (e.g., r^2 LOI MgO = 0.001; r^2 LOI Al_2O_3 = 0.009; r^2 LOI CaO = 0.091; r^2 LOI Na_2O = 0.005; r^2 LOI Ni = 0.007) indicates that these elements were not significantly mobilized even in moderately to highly serpentinized peridotites. To verify this inference, we have plotted an MgO/SiO_2 versus Al_2O_3/SiO_2 diagram (Fig. 3) in which fresh mantle peridotites define the terrestrial array (Jagoutz et al., 1979; Hart and Zindler, 1986). Figure 3 shows that most of the studied mantle peridotites plot close to the terrestrial array, suggesting that serpentinization produced very limited modifications in terms of SiO_2, Al_2O_3, and MgO contents. Most of the samples have Al_2O_3 and CaO contents (Figs. 4A, 4B), as well as Na_2O contents (not shown) plotting close to the theoretical mantle melting curves of Niu (1997), further suggesting that these rocks were not affected by significant addition of these elements during seafloor alteration.

Lherzolites, cpx-poor lherzolites, and harzburgites represent the main rock types identified based on modal composition. Within each rock type, no significant differences can be seen in chemical compositions of samples from different ophiolite massifs in the Albanides and Hellenides (Tables DR1 and DR2). Therefore, each main rock type will be treated as a whole, regardless of the provenance of different samples. The Al_2O_3, and CaO (Figs. 4A, 4B), as well as TiO_2, Na_2O, and Sc (not shown) abundances display well-defined negative correlations with MgO contents. Although less defined (especially in harzburgites), V abundances (Fig. 4C) also show a broad negative correlation with MgO contents. In contrast, Ni (Fig. 4D) and Co (not shown) abundances display positive correlations with MgO contents. The SiO_2, FeO_t, and Cr abundances (~44–46 wt%, ~7–9 wt%, 2000–4000 ppm, respectively) are rather constant at any MgO contents, ranging between ~38 and 49 wt%. Generally, all the studied samples display variably depleted features compared to the depleted MORB mantle (DMM) values (Workman and Hart, 2005).

Lherzolites generally range from slightly depleted to moderately depleted (Al_2O_3 = 4.09–1.32 wt%; CaO = 3.39–1.71 wt%). Compared to cpx-poor lherzolites and harzburgites, all lherzolites have relatively high heavy (H) REE contents with Yb_N = 0.70–2.25 (Figs. 5A, 5B). However, based on middle (M) and light (L) REE contents, two different groups of lherzolites can be identified. Group 1 lherzolites (LREE-depleted lherzolites) display relatively high MREE contents (Sm_N = 0.26–0.92) coupled with highly depleted LREE/MREE ratios (La_N/Sm_N = 0.11–0.41). REE depletion regularly increases from HREE to LREE (Fig. 5A). In contrast, group 2 lherzolites (LREE refertilized lherzolites) have LREE patterns showing abrupt inflections at Nd or Pr (Fig. 5B). In these samples, (La/$Pr)_N$ ratios range from 0.94 to 1.88, whereas (La/$Pr)_N$ ratios, range from 0.57 to 2.06. Such LREE enrichment relative to MREE is commonly interpreted as a result of chromatographic effects associated with melt percolation through peridotites (e.g., Takazawa et al., 1992).

Similar to lherzolites, cpx-poor lherzolites are characterized by LREE/MREE and LREE/HREE depletion (La_N/Sm_N = 0.19–0.27, La_N/Yb_N = 0.02–0.06). However, they show lower REE contents compared with
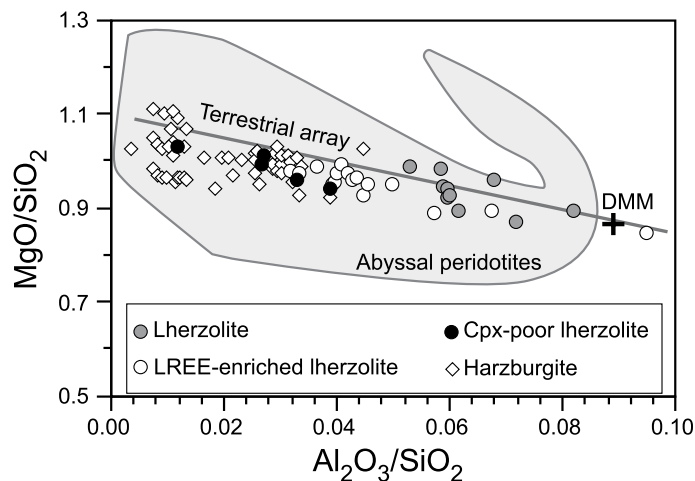
Figure 3. Whole-rock MgO/SiO_2 versus Al_2O_3/SiO_2 diagram for the upper mantle peridotites in the Albanide-Hellenide ophiolites. Major element contents are recalculated to 100% on a loss on ignition–free basis. See Table DR2 for data source of literature-based samples. The terrestrial array is from Jagoutz et al. (1979) and Hart and Zindler (1986). The DMM (depleted mid-oceanic ridge basalt mantle) is from Workman and Hart (2005). Abyssal peridotite data are from PetDB database (http://www.earthchem.org). LREE—light rare earth element; Cpx—clinopyroxene.

lherzolites (Fig. 5A). Their HREE contents are generally lower than those of group 2 (LREE refertilized) lherzolites. However some overlapping REE ranges can be observed in very few samples (e.g., Yb_N = 0.47–1.67 in cpx-poor lherzolites; Yb_N = 0.71–1.14 in group 2 lherzolites; Figs. 5A, 5B). Nonetheless, in contrast to group 2 lherzolites, cpx-poor lherzolites do not show any LREE/MREE enrichment.

Compared to lherzolites, harzburgites generally display higher depletion, although some of them overlap with lherzolite compositions (Fig. 4). Harzburgite compositions reflect a variable refractory nature having very low TiO_2 (<0.06 wt%), Al_2O_3 (0.15–1.99 wt%), and CaO (0.03–2.10 wt%) contents, coupled with high contents of MgO and Ni (Fig. 4). Harzburgites are characterized by U-shaped chondrite-normalized REE patterns with marked depletion of MREE with respect to both LREE and HREE (Fig. 5C). (La/$Sm)_N$ ratios range from ~1–4.58, whereas (Sm/$Yb)_N$ ratios range from 0.04 to 0.27. A few samples from the Bulqiza, Shebenik, and Ypaton ophiolites show a strong depletion in REE contents (ΣREE = 0.08–0.14) compared to other harzburgites (ΣREE = 0.14–0.64), reflecting a highly refractory nature.

The geochemical characteristics of the different groups of mantle peridotites in the ophiolites of the Albanides-Hellenides can be summarized in Figure 6A. The decreasing Al_2O_3/SiO_2 ratio in this figure represents an increasing degree of depletion, whereas the (La/$Nd)_N$ ratios reflect the enrichment in LREE with respect to MREE. Group 1 lherzolites (i.e., LREE-depleted lherzolites) are characterized by a moderate extent of depletion and by (La/$Nd)_N$ ratios generally lower than DMM values. Group 2 lherzolites (i.e., LREE-refertilized lherzolites) show moderate depletion degrees, but (La/$Nd)_N$ ratios generally higher than DMM values. Cpx-poor lherzolites range from moderately depleted to very depleted, and have (La/$Nd)_N$ ratios lower than DMM values. Harzburgites exhibit a depleted to highly depleted nature and are characterized by similar and rather constant (La/$Nd)_N$ ratios. In the Yb_N versus Al_2O_3/SiO_2 diagram (Fig. 6B), all mantle peridotite types show good correlations, implying a strong interrelationship between the HREE contents and the overall compositions of the whole rocks. Yb values regularly decrease as the whole-rock
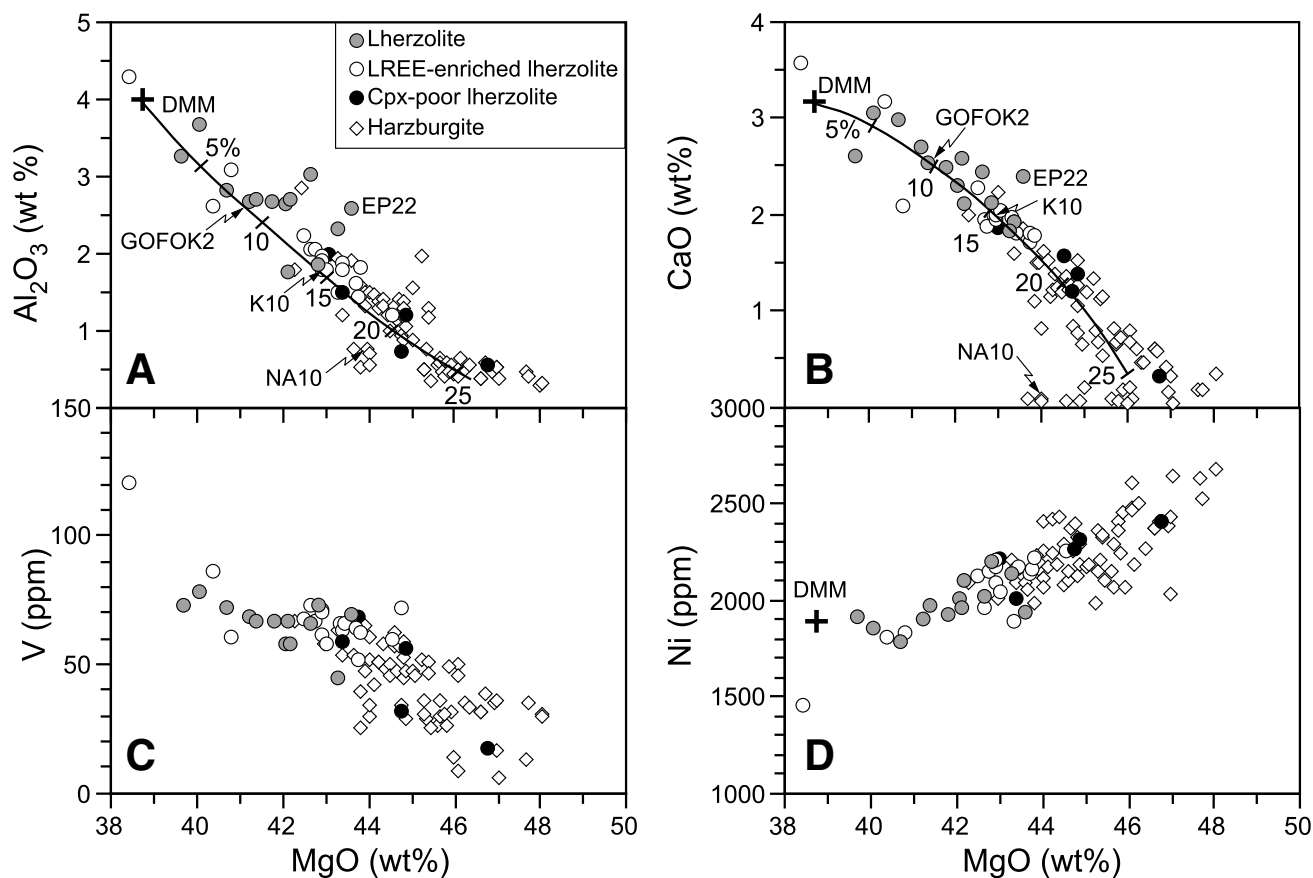
Figure 4. Representative major and trace element contents versus MgO diagrams for whole-rock compositions of the upper mantle peridotites in the Albanide-Hellenide ophiolites. Major element contents are recalculated to 100% on a loss on ignition–free basis. LREE—light rare earth element; Cpx—clinopyroxene. Samples used in the REE models in Figure 9 are also shown. See Table DR2 for data source of literature-based samples. The DMM (depleted mid-oceanic ridge basalt mantle) is from Workman and Hart (2005). Partial melting trends are calculated using the model of Niu (1997). Numbers along the lines indicate percent melting.

depletion increases. However, except cpx-poor lherzolites, the (La/Sm)$_N$ ratios display a negative correlation ($r^2 = 0.85$) with Al_2O_3/SiO_2 ratios (Fig. 6C), suggesting that the LREE/MREE enrichment increases as the whole-rock depletion increases. This is commonly observed in SSZ upper mantle peridotites, particularly in harzburgitic rocks (e.g., Barth et al., 2008; Allahyari et al., 2010, and references therein; Wu et al., 2017). These geochemical features are consistent with slab-derived fluid enrichment of the SSZ mantle source region that had undergone a prior extreme melt-depletion event (Morishita et al., 2011; Uysal et al., 2012; Wu et al., 2017).

Lavas in the Extrusive Sequence

Four different types of volcanic and subvolcanic rocks have been recognized in the Jurassic ophiolites in the Subpelagonian and Pelagonian zones ophiolites of the Albanides-Hellenides (e.g., Shallo, 1994; Beccaluva et al., 1994, 2005; Bortolotti et al., 1996, 2002, 2013; Bébien et al., 2000; Hoeck et al. 2002; Saccani and Photiades, 2004, 2005; Saccani et al., 2004, 2008a, 2008b; Dilek et al., 2005, 2007, 2008): (1) high-Ti basalts showing N-MORB compositions; (2) MTBs; (3) low-Ti IAT basalts, basaltic andesites, andesites, and rhyolites; (4) very low Ti boninitic basalts, basaltic andesites, andesites, and rhyolites. The chemical compositions of volcanic and subvolcanic rocks selected from the literature for this study are presented in Table DR3, together with the relevant references.

High-Ti N-MORBs

Near-primitive Jurassic N-MORBs are found in the WMO, in the Othrys massif, and in the Argolis mélange (Bortolotti et al., 2002; Dilek et al., 2008; Monjoie et al., 2008; Photiades et al., 2003; Saccani and Photiades, 2005). These rocks display a clear subalkaline affinity, as exemplified by their low Nb/Y ratios (0.02–0.09). Their Ti/V ratios range from 26 to 39, clustering in the field of basalts generated at mid-ocean ridge settings (Shervais, 1982). Mg# values [defined as $100 \times Mg/(Mg + Fe^{2+})$] range from 58.8 to 68.1. These overall geochemical features are similar to those of basalts generated at mid-ocean ridges. Relatively primitive basalts (MgO = 7.22–11.62 wt% on anhydrous bases) have TiO_2 = 0.76–2.23 wt%, P_2O_5 = 0.08–0.22 wt%, V = 133–434 ppm, Zr = 48–140 ppm, and Y = 16–59 ppm values. Their FeO_t content ranges from 6.70 to 11.96 wt%. No significant Th and Nb depletions or enrichments with respect to other incompatible elements are observed in the selected samples. Pearce (2008) and Saccani (2015) demonstrated that Th variations with respect to Nb are particularly useful in highlighting subduction input and therefore in discriminating subduction-unrelated from subduction-related magmas. Plotted in a Th-Nb diagram in Figure 7, the Jurassic N-MORBs do not exhibit any detectable subduction influence. N-MORB normalized incompatible element patterns are rather flat with no significant enrichment or depletion in Th, Ta, Nb, P, and Zr (Fig. 8A). REE patterns (Fig. 8B) show depletions in LREEs with respect
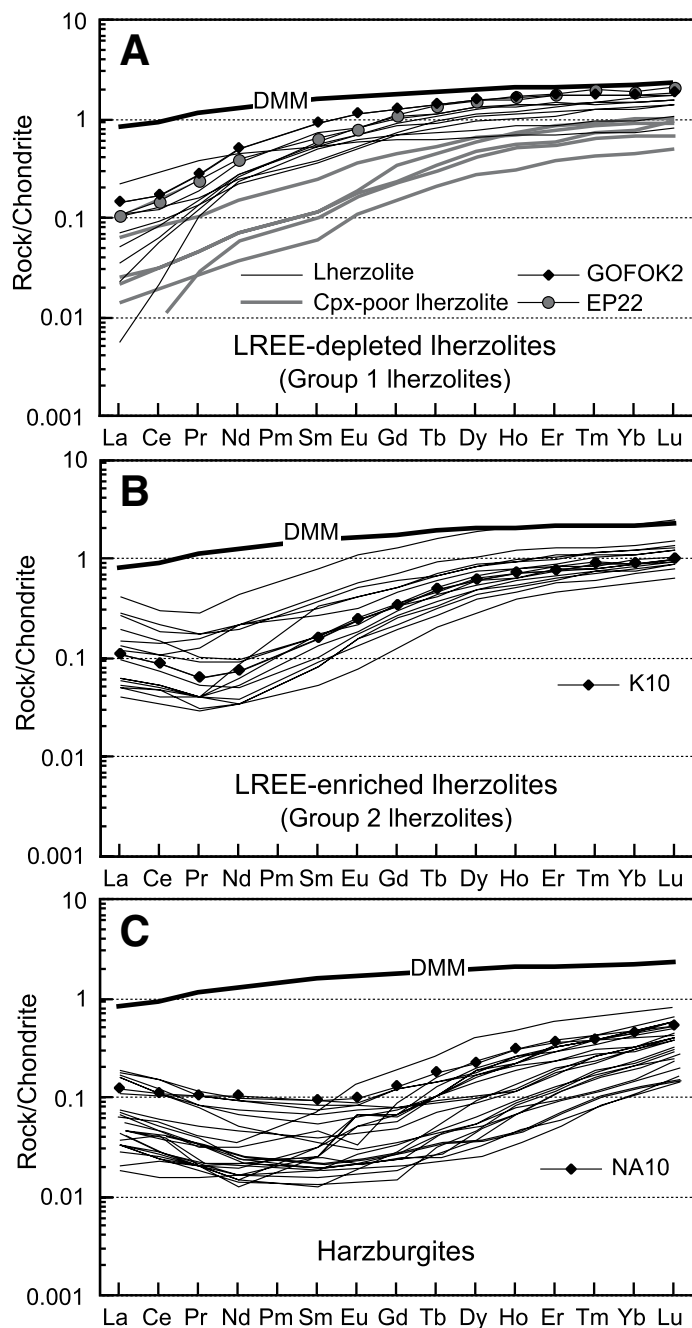
Figure 5. Chondrite-normalized rare earth element (REE) (L—light) composi-
tions of the upper mantle peridotites in the Albanide-Hellenide ophiolites.
See Table DR2 for data source of literature-based samples. Samples used
in the REE models in Figure 9 are also shown. Normalizing values are from
Sun and McDonough (1989). The composition of the depleted mid-
oceanic ridge basalt mantle (DMM) is from Workman and Hart (2005).
Cpx—clinopyroxene.
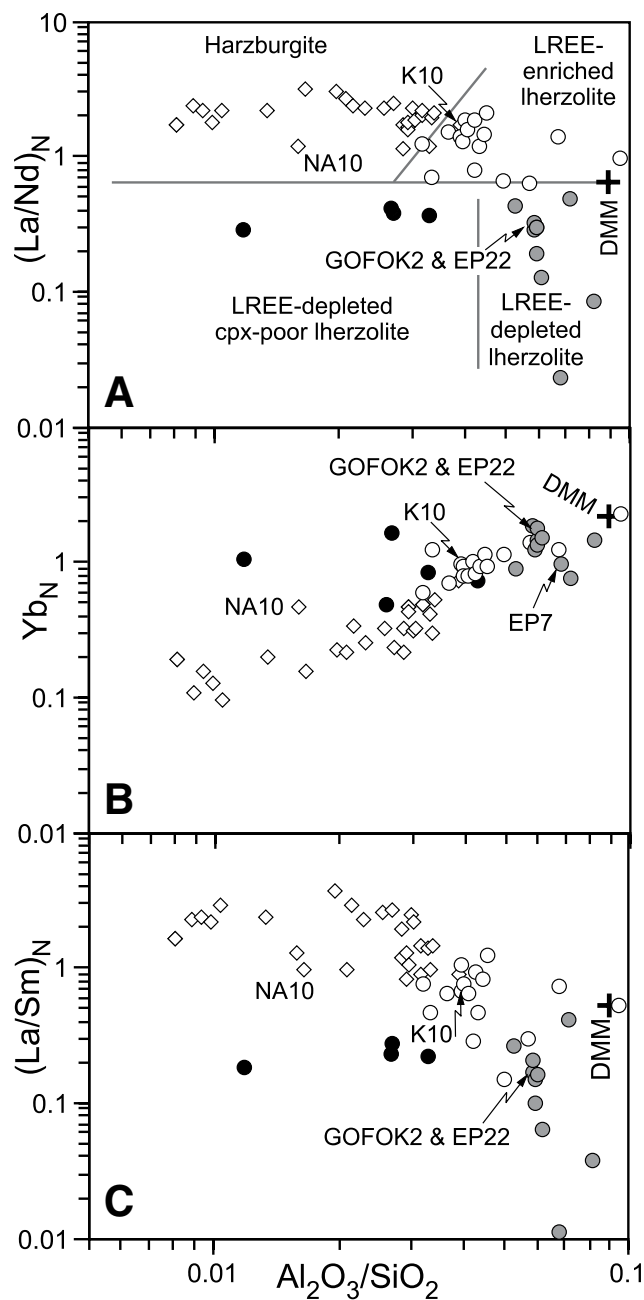
Figure 6. (A) Variations of $(La/Nd)_N$ versus Al_2O_3/SiO_2 based on whole-rock
compositions of the upper mantle peridotites in the Albanide-Hellenide
ophiolites. LREE—light rare earth element; cpx—clinopyroxene; DMM—
depleted mid-oceanic ridge basalt mantle. (B) Yb_N versus Al_2O_3/SiO_2. (C)
$(La/Sm)_N$ versus Al_2O_3/SiO_2. Samples used in the rare earth element (REE)
models in Figure 9 are also shown. See Table DR2 for data source of liter-
ature-based samples. Normalizing values are from Sun and McDonough
(1989). The DMM composition is from Workman and Hart (2005).
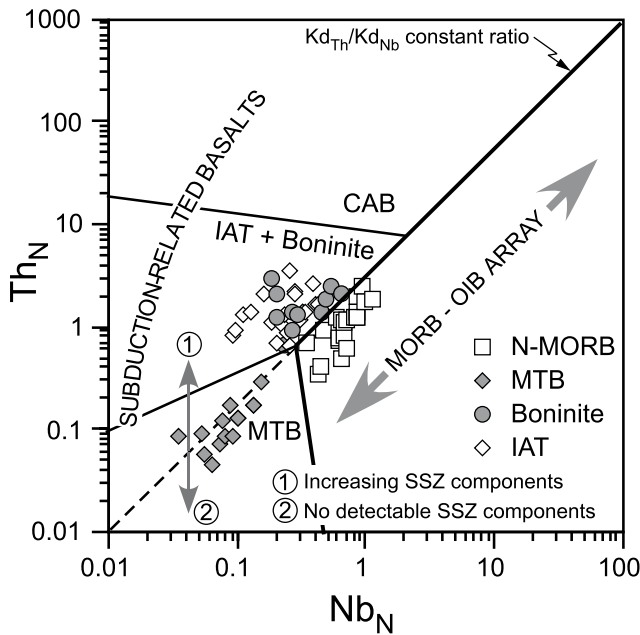
Figure 7. Normal mid-oceanic ridge basalt (N-MORB) normalized Th versus Nb diagram (modified from Saccani, 2015) for the Jurassic, near-primitive basalts from the Albanide-Hellenide ophiolites. See Table DR3 for data source. Normalizing values are from Sun and McDonough (1989). N-MORB is high-Ti. Abbreviations: MTB—medium-Ti basalt; IAT—island arc tholeiitic basalt (low-Ti); CAB—calc-alkaline basalt; SSZ—suprasubduction zone.

to MREEs and HREEs, as evidenced by the $(La/Sm)_N$ (0.41–0.78) and $(La/Yb)_N$ (0.34–0.86) ratios.

MTBs

The MTBs crop out in the WMO of the northern and southern Albanides, the Pindos massif, and as blocks included in the Rubik and Othrys mélanges (Bortolotti et al., 2002; Hoeck et al., 2002; Photiades et al., 2003; Saccani and Photiades, 2005). These basaltic rocks show geochemical characteristics between those of MORBs and IATs (Bébien et al., 2000; Saccani et al., 2011; Saccani, 2015). In comparison to MORB, near primitive MTBs (MgO = 6.92–13.90 wt% on anhydrous bases) show comparable or slightly lower contents in TiO_2 (0.67–1.09 wt%), P_2O_5 (0.01–0.17 wt%), Zr (5–90 ppm), and Y(18–29 ppm). Their Ti/V ratios (16–28) straddle the boundary between the IAT and MORB fields (Shervais, 1982), and their Mg# values are relatively high (Mg# = 75.8–61.2). Co (39–65 ppm), Ni (67–296 ppm), and Cr (211–656 ppm) contents are higher than those observed in MORBs at comparable degrees of fractionation, suggesting a relatively more refractory nature of their mantle source.

The contents of high field strength elements (HFSE) are slightly lower than those of N-MORBs with comparable degrees of fractionation, but Th, Ta, and Nb contents are highly depleted with respect to those of MORBs (Fig. 8C). Their Th and Nb values are ~0.1 times N-MORB composition, and are significantly lower than those of IAT and boninitic basalts (Fig. 7). They display no Th enrichment with respect to Nb, indicating no detectable subduction-related contribution (Saccani, 2015); in Figure 7, they plot below the line delineating Th enrichment relative to Nb (enrichment-depletion array). Accordingly, MREE and HREE compositions are slightly lower than those of N-MORBs, but LREE values are highly depleted with respect to those of MORBs (Fig. 8D). The $(La/Sm)_N$ and $(La/Yb)_N$ ratios are in the range of 0.02–0.29 and 0.01–0.25, respectively.

Low-Ti IAT Basalts

Near-primitive IAT basalts are rather rare in the Albanide-Hellenide ophiolites, where IAT rocks are largely represented by fractionated products, such as andesites and basaltic andesites. Samples selected for this study are from the EMO in the northern Albanides and the Vourinos massif (Dilek et al., 2008; Saccani et al., 2008b), except one sample that was collected in the WMO in the northern Albanides (see Dilek et al., 2008). Near-primitive IAT basaltic rocks (MgO = 7.04–10.42 wt% on anhydrous bases) have relatively low TiO_2 contents (0.48–1.10 wt%) and low Ti/V ratios (9–18). They also have relatively low contents of P_2O_5 (0.04–0.06 wt%), Zr (18–56 ppm), and Y (11–30 ppm), combined with variable amounts of Al_2O_3 (13.59–16.70 wt%), FeO_t (8.38–10.69 wt%), Cr (22–345 ppm), and Ni (18–157 ppm). Mg# values in basalts range from 68.1 to 60.7. N-MORB–normalized HFSEs exhibit depleted patterns ranging from 0.3 to ~1.0 × N-MORB compositions, and display mild negative anomalies in Th, Ta, and Nb (Fig. 8E). They show a clear Th enrichment with respect to Nb, suggesting subducting slab influence (Fig. 7). These rocks are characterized by depletion in LREEs (Fig. 8F), as exemplified by the $(La/Sm)_N$ (0.35–0.76) and $(La/Yb)_N$ (0.20–0.63) ratios.

### Very Low Ti Boninitic Basalts

Very low Ti boninitic rocks are widespread in the Albanide-Hellenide ophiolites, and are mainly represented by basaltic andesites and andesites, whereas near-primitive boninitic basalts are volumetrically subordinate. The near-primitive basaltic rocks (MgO = 8.50–19.18 wt% on anhydrous bases) examined in this study are from both WMO and EMO (Bortolotti et al., 2002; Dilek et al., 2008) and Pindos (Saccani and Photiades, 2004), as well as from Koziakas, Othrys, Argolis, and Vermion mélange units (Saccani et al., 2003, 2008a; Photiades et al., 2003; Saccani and Photiades, 2005). These boninitic rocks are characterized by very low TiO_2 contents (0.12–0.46 wt%) and Ti/V ratios (4–11), which are comparable with those of typical boninitic rocks from forearc regions of oceanic island arcs (e.g., Crawford et al., 1981, 1989). Their P_2O_5 (<0.10 wt%), Zr (<36 ppm), and Y (<11 ppm) contents are very low, reminiscent of typical boninitic compositions, and their Mg# values are relatively high (82.0–67.6). High Mg# values are common in boninitic rocks from modern oceanic settings (e.g., Dobson et al., 2006). The Al_2O_3 and FeO_t contents are highly variable (8.55–17.39 wt% and 5.16–9.20 wt%, respectively), as are their MgO and CaO contents. However, in many samples these values can reach very high contents (i.e., MgO to ~20 wt% and CaO to ~12 wt%, respectively). Compatible element contents, such as Ni (to 869 ppm) and Cr (to 1739 ppm), are also relatively high.

Very low Ti boninitic basalts are strongly depleted in HFSE, whereas Rb, Ba, and Th are fairly enriched with respect to typical N-MORB (Fig. 8G). We recognize, however, that the large variabilities in their Rb and Ba values possibly reflect secondary alteration effects. The selected samples display U-shaped REE patterns typical of boninites (Fig. 8H), with $(La/Sm)_N$ = 1.03–2.85 and $(Sm/Yb)_N$ = 0.25–0.78. Similar to IAT basalts, they show a clear Th enrichment with respect to Nb, suggesting subducted slab influence (Fig. 7).

MANTLE PERIDOTITE EVOLUTION AND FORMATION OF PRIMARY MAGMA TYPES: PETROGENETIC CONSTRAINTS

Mantle Source, Primary Magma Generation, Mantle Residua: REE and Cr-Y Modeling

Compositions of both mantle peridotites and near-primitive basalts can be used to constrain the mutual relationships among the mantle source, primary magma generation, and mantle residua during the evolution of the
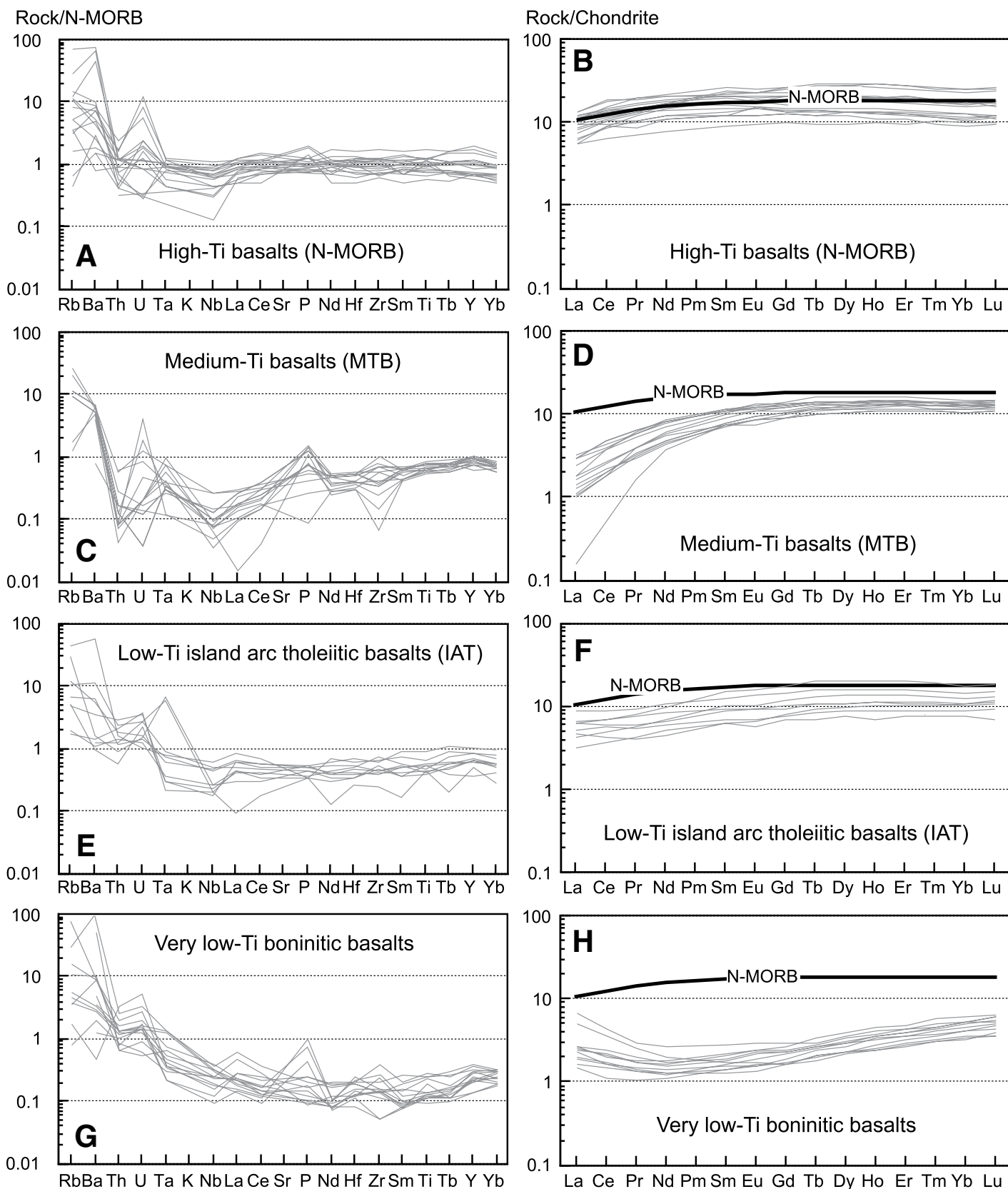
Figure 8. Normal mid-oceanic ridge basalt (N-MORB) normalized incompatible element compositions (left column) and chondrite-normalized rare earth element (REE) compositions (right column) of the Jurassic near-primitive basalts from the Albanide-Hellenide ophiolites. See Table DR3 for data source. Normalizing values and the composition of typical N-MORB are from Sun and McDonough (1989).

Jurassic oceanic lithosphere preserved in the Albanide-Hellenide ophiolites, in particular to deduce the possible mantle sources and their degree of melting. The simplest way to constrain these mutual relationships is to model REE abundances. An alternative method is to plot a compatible (e.g., Cr) versus an incompatible element (e.g., Y). Compatible element abundance is not significantly modified during the progressive mantle source depletion, whereas abundance of incompatible elements is closely related to source depletion and degree of melting (Pearce, 1982; Murton, 1989; Kostopoulos and Murton, 1992). We assume that the different mantle peridotites in these ophiolites likely represent either the mantle melt source or the mantle residua associated with the formation of different magma types.

We have applied REE and Cr-Y modeling in order to find the mantle peridotite compositions that best fit both the melt and residual peridotite compositions for each magmatic type. The internal structure, petrology, and geochemistry of intrusive and extrusive rocks of the Albanide-Hellenide ophiolites display a magmatic progression (from west to east and throughout time) from N-MORB to MTB, IAT, and boninitic compositions, as demonstrated by recent studies (Dilek et al., 2007, 2008; Phillips-Lander and Dilek, 2009; Saccani et al., 2011). These spatial and temporal relationships are significant to examine the time-progressive evolution of ophiolitic magmas with respect to their potential mantle melt sources. Therefore, we have also used REE and Cr-Y modeling to test whether the mantle residua left after a particular magmatic event could have potentially made up the mantle source for the subsequent episode of magmatism recorded in the ophiolite sequences.

In this study we postulate nonmodal batch partial melting for MORB and MTB rocks and fractional melting for IAT and boninitic rocks. The application of these models is dependent on two critical assumptions: (1) the initial peridotite does not undergo any other process apart from partial melting and instantaneous melt removal, and (2) the mantle source has a uniform composition. However, many modeling studies of peridotites have shown that neither of these assumptions is fully valid because of melt-rock interactions, fluid-influenced refertilization of the mantle source, and subsolidus reequilibration of mantle mineral assemblages. It has been demonstrated that melts produced in both mid-ocean ridge and SSZ settings commonly react with the peridotites during their extraction (e.g., Lambart et al., 2012; Brunelli et al., 2014), as their migration through the mantle results in various forms of melt-rock interaction. Melt transport may occur in channels that allow high melt fluxes (e.g., Kelemen et al., 1995; Elliott and Spiegelman, 2003), or alternatively it may occur at grain boundaries, causing porous flow and related melt-rock interaction (e.g., Dijkstra et al., 2003; Barth et al., 2008). The melt-rock interactions encompass a wide range of processes, from simple melt crystallization with decreasing temperatures to open system melting, whereby the host peridotite is both melting and reacting with a migrating melt (see Warren, 2016, for an exhaustive discussion).

In SSZ settings, the previously depleted mantle peridotites are commonly refertilized by fluid-mobile trace elements, such as LREEs and Th, and by slab-derived fluids (e.g., Gribble et al., 1996; Parkinson and Pearce, 1998). The extent and timing of fluid-induced refertilization are difficult to constrain, because the fluid flux from a subducted slab may be either localized or pervasive. Moreover, fluid-mobile trace elements may be added at every melting increment (see Barth et al., 2003, 2008). In addition, compositions and the amounts of subduction-related trace elements incorporated into the overlying mantle wedge depend on a number of factors, such as the mineralogical compositions of the subducting rocks (in turn, mostly depending on their alteration degrees as highly versus little serpentinized peridotites and spilitized basalts), temperatures, pressures, and distance from a subduction zone (Pearce and Parkinson, 1993; Pearce and Peate, 1995; Gribble et al., 1996; Taylor and Martinez, 2003;

Dilek and Furnes, 2009, 2014). Different trace element enrichments are associated with the nature of fluids released from subducted crust and felsic magmas generated by partial melting of subducted sediments (e.g., Macdonald et al., 2000). The trade-off between the rate of extensional tectonics in the upper slab and the slab rollback is also important in facilitating fluid transfer (e.g., Dilek and Flower, 2003; Flower and Dilek, 2003).

Given these uncertainties, a rigorous quantification of partial melting processes is not possible, particularly if they are investigated at a regional scale, as in our study. However, semiquantitative modeling of the REE and Cr-Y covariation by using batch partial melting and fractional melting models can represent simplified end-member scenarios for the generation of melts at both mid-ocean ridges and SSZ settings. The results may then provide a first-order fit for the trace element compositions of residual peridotites. The REE modeling is mainly focused to reproduce MREE and HREE (i.e., Sm through Yb) abundances, as LREE (i.e., La through Pm) abundances are more influenced by melt-rock or fluid-rock interactions, as well as by secondary alteration and metasomatism. The results of our REE and Cr-Y modeling are shown in Figures 9 and 10, respectively; the modal compositions of the assumed mantle sources, the melting proportions and the trace element distribution coefficients used herein are provided in Table DR5.

N-MORB

The low Zr/Y ratios (2–3.4) shown by the near-primitive N-MORBs in the Albanide-Hellenide ophiolites indicate that these rocks likely originated from partial melting of primary mantle sources (Zr/Y < 4; Pearce and Norry, 1979). The very low Ta/Yb ratios (0.01–0.08) are generally compatible with a genesis from a depleted N-MORB–type suboceanic mantle source, with no influence of enriched ocean island basalt material. For REE modeling, we consider the DMM composition of Workman and Hart (2005) as the possible mantle source for the near-primary N-MORBs. The melting model (Fig. 9A) shows that the near-primitive N-MORBs are generally compatible with 10%–20% partial melting of a DMM source. The calculated mantle residua for such degrees of partial melting fit well with the REE contents of the lherzolites exposed mainly in the westernmost Pindos and Othrys ophiolites, but also in the Kallidromon area. Similar conclusions are obtained from the Cr-Y modeling depicted in Figure 10A. In this plot, the depleted mantle (DM) composition of Salters and Stracke (2004) is assumed as the possible mantle source for the near-primary N-MORBs because no Cr content is given for the DMM. Figure 10A shows that the Cr-Y covariation in the near-primitive N-MORBs is compatible with 10%–15% partial melting of a DM source. The calculated mantle residua are well represented by lherzolitic compositions. We therefore conclude that these lherzolites may represent the mantle residua left after N-MORB type melt extraction during the early petrogenetic evolution of the Jurassic Tethyan oceanic lithosphere in the region.

MTB

The near-primitive MTBs have LREE values (Fig. 8D) and Zr/Y ratios (0.2–1.8), as well as Th and Nb contents that are significantly lower than those of MORBs (Fig. 7). These features suggest that MTBs were originated from partial melting of mantle sources, which were more refractory with respect to a MORB source (see Saccani et al., 2011; Saccani, 2015). Therefore, we postulate that the mantle sources of these MTBs are represented by those lherzolites left as the residual mantle after the initial N-MORB melt extraction. In both our REE and Cr-Y modeling (Figs. 9B and 10A) a lherzolite from the Pindos massif (Saccani and Photiades, 2004) has been considered as the possible mantle source (sample EP22; Table DR2). The REE composition of MTBs is compatible with low degrees of partial melting (~5%–8%) of this Pindos lherzolite. The
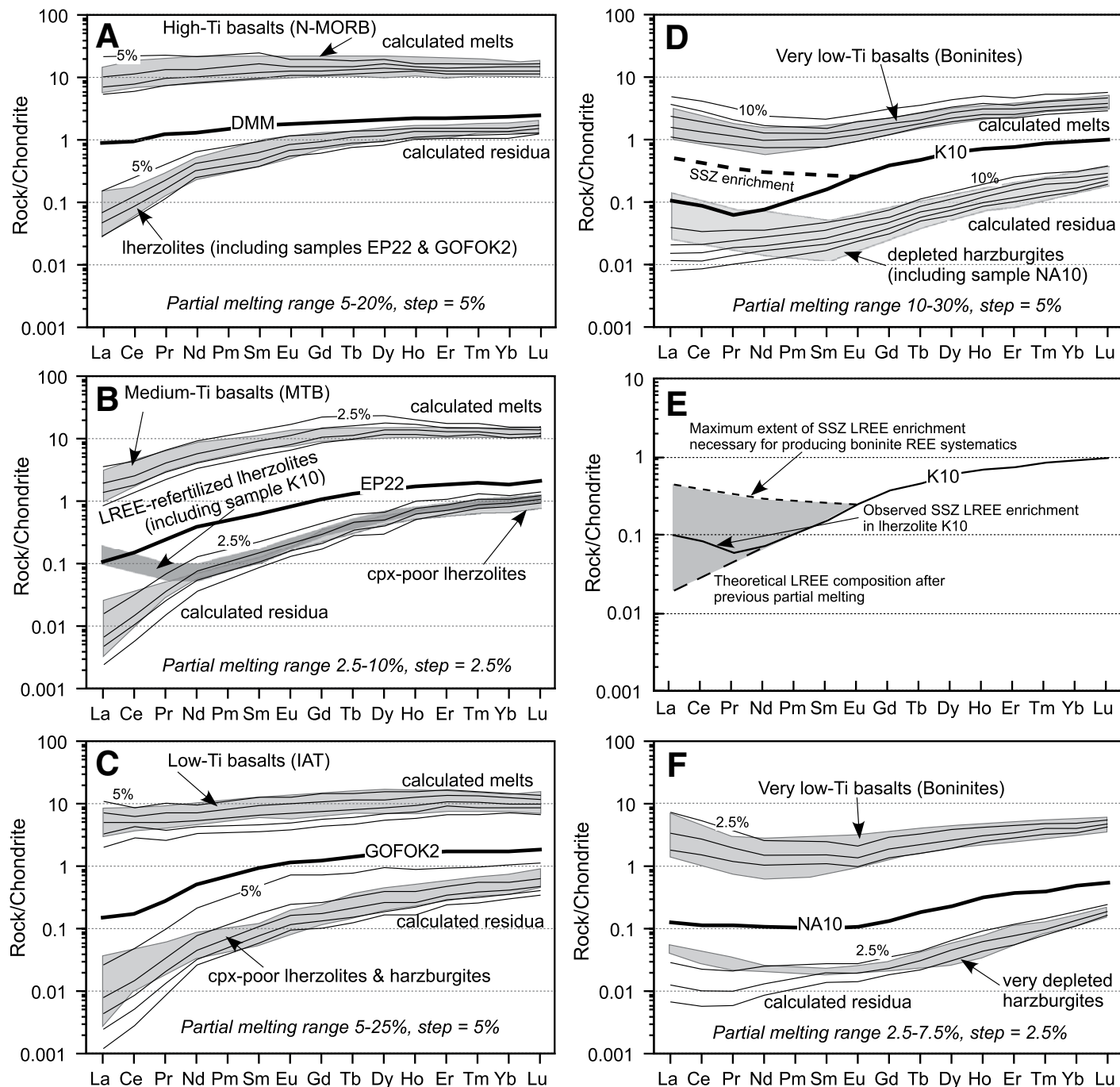
Figure 9. Calculated chondrite-normalized (Sun and McDonough, 1989) rare earth element (REE) (L—light) patterns for parental melts and complementary residua derived from different mantle sources, assuming various degrees of partial melting according to the parameters listed in Table DR5. Gray fields encompass the compositional variations of near-primitive basalts, as well as of the upper mantle peridotites from the Albanide-Hellenide ophiolites. N-MORB—normal mid-oceanic ridge basalt; DMM—depleted mid-oceanic ridge basalt mantle; cpx—clinopyroxene; SSZ—suprasubduction zone.
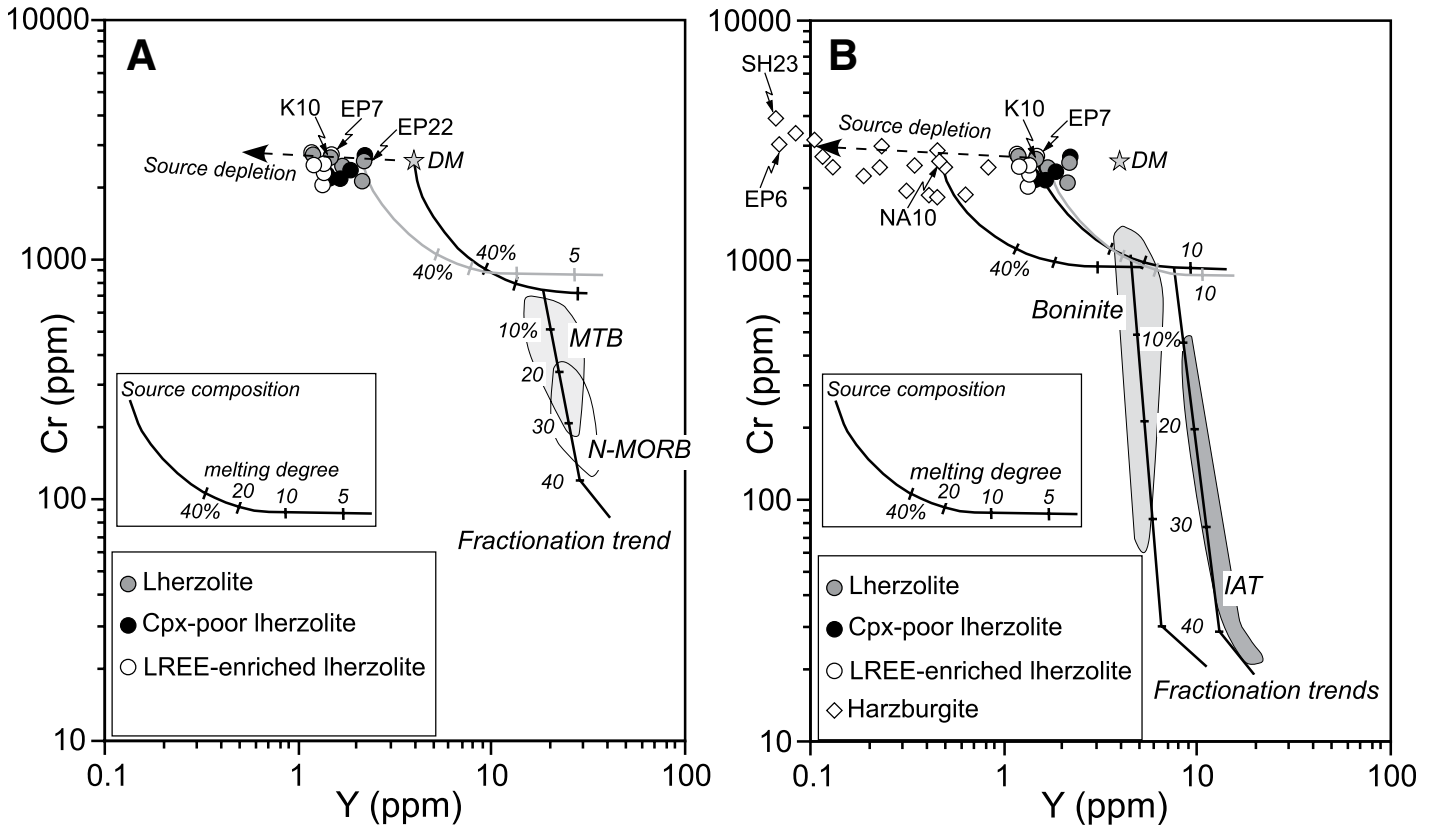
Figure 10. Cr versus Y diagram (modified after Pearce, 1982) for upper mantle peridotites in the Albanide-Hellenide ophiolites; also shown are melting paths starting from different mantle peridotite compositions. Gray fields represent the extents of chemical variations for near-primitive normal mid-oceanic ridge basalt (N-MORB), medium-Ti basalt (MTB), low-Ti island arc tholeiite basalt (IAT), and very low Ti boninitic basalt from the Albanide-Hellenide ophiolites. (A) Melting paths for N-MORB and MTB. LREE—light rare earth element; cpx—clinopyroxene; DM—depleted mantle. (B) Melting paths for IAT and boninitic basalts. Mantle source compositions and melting parameters are listed in Table DR5. The composition of the depleted MORB-type mantle source is from Salters and Stracke (2004).

marked LREE depletion with respect to MREE of this presumed mantle source suggests that it did not undergo any subsequent LREE enrichment by subduction-related fluids. The calculated residua for ~5%–8% partial melting fit well with the REE compositions of the cpx-poor lherzolites from the Othrys and Kallidromon ophiolites, particularly for their MREE and HREE contents, as well as those of the LREE-refertilized lherzolites with relatively low cpx contents (i.e., 8%–9%) from the same ophiolitic massifs. Such a close compositional similarity between these lherzolites and the calculated residua (Fig. 9B) suggests that these mantle rocks likely represent the residual mantle composition left behind after MTB melt extraction. The high LREE contents in the LREE-refertilized lherzolites compared to the calculated residua is most likely due to LREE refertilization that may have occurred after the melting event. Accordingly, Figure 10A shows that the Cr-Y contents of MTBs are compatible with 5%–10% partial melting of the same lherzolite sample (EP22) used for the REE modeling. The calculated Cr and Y residual contents are similar to those observed in lherzolites from the Pindos (e.g., sample EP7) and Kallidromo (e.g., sample K10) areas. The Cr-Y modeling in Figure 10A shows that MTB compositions can also be compatible with 15%–20% partial melting of a DM source. However, such a high degree of partial melting of this source cannot explain the REE compositions of these rocks.

Sample EK1a from the Othrys mélange shows an extreme depletion in LREEs (Fig. 8D; Table DR3) that cannot be explained by the above model. Such LREE depletion implies a comparable depletion in the mantle

source. Within our data set, only the lherzolite EP7 from Pindos (Table DR1) displays a very marked LREE depletion. Taking this lherzolite as a possible mantle source, our REE modeling shows that the REE contents of sample EK1a are perfectly compatible with 5% partial melting of the assumed mantle source (not shown). However, the calculated residua do not fit with any of the mantle peridotites in our data set.

Low-Ti IAT

IAT near-primitive basalts have REE values (Fig. 8F) and Zr/Y ratios (<2) that are consistent with an origin from partial melting of refractory mantle sources. Their Th enrichment relative to Nb suggests an arc signature (Dilek et al., 2008; Saccani et al., 2011; Saccani, 2015). However, the slightly LREE-depleted nature of these basalts suggests that hydration of the SSZ mantle wedge was accompanied by a moderate transfer of LREE-enriched subduction zone components (e.g., Saccani et al., 2004; Barth et al., 2008). Therefore, we posit a residual MORB mantle lherzolite, which was slightly enriched in La and Ce by subduction-derived fluids, as the possible mantle source for IAT basalts (sample GOFOK2 from the Othrys ophiolite; Barth et al., 2008).

Figure 9C shows that chondrite-normalized REE patterns of the near-primitive basalts are consistent with ~10%–20% partial melting of this lherzolite. The calculated MREE and HREE abundances in the residual peridotite are comparable with those of some depleted (i.e., cpx poor) lherzolites and harzburgites from various localities. However, the predicted

LREE compositions are ~3–5 times lower than the observed compositions. This feature can be explained by LREE enrichment of the mantle peridotites as a result of various types of melt-rock interactions (see Warren, 2016; Wu et al., 2017) or in situ crystallization of small volumes of low-degree melts (Dijkstra et al., 2003; Brunelli et al., 2014). Some amounts of LREE refertilization of the mantle residua (i.e., after the melting event) by subduction-derived fluids cannot be ruled out. Despite the discrepancy between the predicted and the observed LREE contents, the calculated values of MREEs and HREEs are in agreement with the geochemistry of the depleted lherzolites and harzburgites from the Othrys and Kallidromon ophiolites. Therefore, these rocks can be assumed to represent the residual mantle, left after IAT melt extraction. Although we select lherzolite sample EP7 from the Pindos massif on the Cr-Y plot in Figure 10B, because no Y content is available for the sample GOFOK2 used for REE modeling, this diagram fully supports this conclusion. The Cr-Y covariation in the near-primitive IAT basalts is compatible with the calculated composition for ~15% partial melting of this lherzolite. The calculated Cr and Y residual contents are similar to those observed in many harzburgites from various localities of the Albanide-Hellenide ophiolites.

Very Low Ti Boninitic Basalts

The boninitic near-primitive basalts show more pronounced REE depletions coupled with marked LREE/MREE enrichments when compared to MTBs and IATs (Fig. 8H). These features are commonly attributed to a high degree of partial melting of progressively depleted mantle sources, which were variably but significantly enriched in LREEs by subduction-derived fluids (e.g., Pearce, 1982; Beccaluva and Serri, 1988). However, none of the mantle peridotites within our data set can match these features. Thus, in the REE modeling shown in Figure 9D we have taken as a possible mantle source the LREE-refertilized lherzolite K10 from the western Othrys ophiolite. As shown herein, this rock may represent the mantle residuum after 10%–15% N-MORB–type melt extraction, followed by 5%–8% MTB-type melt extraction (Fig. 9B). However, although this rock was likely slightly refertilized in LREEs, the LREE values in both calculated melts and the mantle residua would be much lower than those observed in boninitic basalts and mantle harzburgites, respectively, when we use its composition. For this reason, a theoretical LREE enrichment of sample K10 has been postulated in Figure 9D. The calculated REE compositions for high degrees of partial melting (15%–25%) of the lherzolite sample K10 with modified LREE contents fully correspond to the REE compositions of many boninitic basalts from the Pindos, Argolis, and Vermion ophiolites. The MREE and HREE compositions of the calculated residua correspond to those of many harzburgites and depleted harzburgites from the Othrys (this study; Barth et al., 2008), Vermion (Saccani et al., 2008a), and Ypaton ophiolites.

The maximum amount of LREE enrichment in a SSZ setting can be roughly estimated (Fig. 9E). The maximum amount of LREE enrichment is given by the difference between the theoretical LREE content that is necessary for fitting boninite compositions and the theoretical LREE composition of the lherzolite sample K10 without considering the LREE/MREE enrichment observed in this sample. The theoretical La content after the maximum extent of LREE is ~20 times that of the lherzolite residual after previous melt extraction. This estimated value can reasonably be assumed to represent the order of magnitude of LREE enrichment in a forearc mantle. Modeling using the Cr-Y covariation shows that the compositions of the near-primitive boninitic basalts are compatible with ~25% partial melting of the same lherzolite sample (K10) used for the REE modeling. The calculated Cr and Y residual contents are similar to those observed in highly depleted harzburgites from different localities (e.g., sample NA10 from the Vermion massif).

The Albanide-Hellenide ophiolites also include highly depleted harzburgites showing very low HREE contents (Fig. 5C; Tables DR1 and DR2) and very low Al_2O_3/SiO_2 ratios (Fig. 6), which cannot be explained by the REE model described here. Beccaluva et al. (2005) suggested that primary boninitic lavas in the Albanide-Hellenide ophiolites might have also been generated by lower (<10%) degrees of partial melting of a refractory harzburgitic mantle source residual after the extraction of MTB and/or IAT primary melts, but significantly enriched in LREEs. Therefore, in the model depicted in Figure 9F, a refractory harzburgite from the Vermion ophiolites that represents the mantle residuum after boninitic melt extraction (sample NA10) has been assumed as an alternative mantle source for boninitic magma generation. The REE contents in predicted melts for 2.5%–7.5% partial melting of this refractory harzburgite overlap with those of some boninitic basalts (especially those showing the highest LREE/MREE ratios) from the northern Mirdita, Othrys, and Argolis ophiolites (Dilek et al., 2008; Saccani et al., 2003; Saccani and Photiades, 2005). The MREE and HREE values of the highly depleted harzburgites from the central Mirdita, Vourinos (Saccani and Photiades, 2004; Barth et al., 2008), and Ypaton ophiolites (Tables DR1 and DR2) are generally compatible with the calculated mantle residua.

The predicted residual LREE compositions of the boninitic basalts do not fit well; however, the LREE contents observed in the mantle peridotites do, as was the case for the IAT basalts (Figs. 9D, 9E), and they are ~3–5 times lower than the observed compositions. We can explain this discrepancy by an LREE enrichment of the mantle peridotites resulting from various types of melt-rock interaction (see Warren, 2016) or by in situ crystallization of small volumes of low-degree melts (Dijkstra et al., 2003; Brunelli et al., 2014). Alternatively, LREE refertilization of the mantle residua from subduction-derived fluids can also explain the LREE contents in the mantle harzburgite that are higher than those in the calculated residua. Results from Cr-Y modeling (Fig. 10B) are in good agreement with those obtained from REE modeling. The Cr-Y composition of some boninites is compatible with ~5% partial melting of the same harzburgite sample NA10 used for the REE modeling. The calculated Cr and Y residual contents are similar to those observed in extremely depleted harzburgites from the Bulqiza (e.g., sample SH7) and Pindos massifs (e.g., sample EP6).

Subduction Initiation and Melt Evolution

The upper mantle peridotites exposed in the Albanide-Hellenide ophiolites represent the remnants of a mantle source, which underwent multiple, time-progressive melting episodes, as discussed in the following.

1. Moderately depleted lherzolites showing LREE and/or MREE depletion represent a mid-ocean ridge–type mantle and are compositionally complementary to the high-Ti basalts found in the western-type (WMO) ophiolites.

2. These lherzolites may represent suitable mantle source rocks for the MTBs, also found in the western-type volcanic sequences. MTBs are compatible with ~5%–8% partial melting of a mantle source, previously depleted by ~15%–20% MORB melt extraction without addition of subduction-derived fluids (see also Photiades et al., 2003; Saccani et al., 2011). The depleted cpx-poor lherzolites displaying marked LREE and/or MREE depletion, and exposed mainly in the WMO ophiolites, represent the complementary residua of MTBs.

3. The LREE-enriched lherzolites that are widespread in the western-type ophiolites represent a SSZ-type mantle. They are moderately depleted and have MREE and HREE compositions compatible with those of MORB-type mantle residua. However, they show variable but generally moderate amounts of La-Ce enrichment, which points to the

addition of slab-derived fluids from a subducting Tethyan lithosphere. These lherzolites may be the suitable mantle source for the IAT basalts of the eastern-type (EMO) volcanic sequences. The mantle residua that are complementary to the IAT basalts are represented by depleted, cpx-poor lherzolites and harzburgites.

4. The depleted harzburgites, typically characterizing the eastern-type upper mantle units but also cropping out in the western-type Pindos and Othrys ophiolites, represent a typical SSZ-type mantle similar to the peridotites documented from the IBM forearc (e.g., Pearce et al., 1992). These harzburgites are the complementary residua to the boninitic basalts produced by high degrees of partial melting of the IAT-type or MTB-type mantle residua, which were significantly enriched in LREEs by SSZ-type fluids. Highly depleted harzburgites occurring in the EMO and Vourinos may represent the complementary residua after low degree (~5%) partial melting of the refractory harzburgites.

Our melt modeling results show that the depleted cpx-poor lherzolites are residual after MTB-type melt extraction, and that their chemical features are best explained by low-degree melting of mantle sources that underwent previous MORB-type melt extraction. These residual lherzolites were subsequently enriched in LREEs by subduction-derived fluids and became the mantle sources of IAT and boninitic magmas. Implicit in this interpretation is that MORB-type magmatism predated the SSZ-type magmatism during the ophiolite evolution. However, the occurrence in the field of alternating MORB and MTB volcanic flows in the WMO and in the Pindos ophiolites and the existence of MORB-type mafic-ultramafic cumulates associated with highly refractory mantle harzburgites or boninitic-type mafic-ultramafic cumulates in the Bulqiza, Shebenik, southern Albanides and Othrys ophiolites (Bortolotti et al., 2002; Bébien et al., 1998; Hoeck et al., 2002; Saccani and Photiades, 2004; Barth et al., 2008) indicate that MORB magmatism was not only associated with the eruption of MTBs during the infancy of intraoceanic subduction, but also persisted locally, at least until the IAT magmatic stage (Barth et al., 2008). Microstructural and geochemical studies of the plagioclase peridotites in the Othrys ophiolite show that these rocks formed as a result of impregnation of refractory harzburgites with a fractionating MORB-type melt (Dijkstra et al., 2003; Barth et al., 2003), and these findings are consistent with our interpretation of the coeval evolution of MORB-type magmatism with both the MTB and IAT volcanism.

Formation of MTBs by partial melting of lherzolites, which were residual after ~20% MORB-melt extraction, without any addition of subduction-derived fluids and components requires an anomalously high thermal regime (Bébien et al., 2000; Insergueix-Filippi et al., 2000). Such a high thermal regime is also necessary for the generation of boninitic melts from high-degree partial melting of refractory mantle sources at subduction initiation (Falloon and Danyushevsky, 2000). These thermal conditions led some researchers to propose subduction initiation at a ridge axis (Bébien et al., 2000; Insergueix-Filippi et al., 2000; Bortolotti et al., 2002; Barth et al., 2008), where asthenospheric upwelling provides anomalously high heat. The results of numerical modeling studies have shown that initiation of subduction at a ridge axis does not immediately halt the MORB-type asthenospheric flow, but may push this flow in the same direction as the lithospheric subduction (Insergueix-Filippi et al., 2000). This process helps the preservation of high temperatures in the mantle of the upper plate and triggers partial melting, which results in the production of MTB and boninitic magmas during the earliest stages of subduction initiation. This magmatic episode overlaps with progressively extinguishing MORB-type volcanism. However, slab failure and subduction initiation along a hot, thin, and buoyant mid-ocean ridge system is potentially a difficult geodynamic conversion and may require significant changes in the stress regime within and around the seafloor spreading system.

To get around this problem, Maffione et al. (2015) and van Hinsbergen et al. (2015) proposed that oceanic detachment faults, which are generally parallel to mid-ocean ridge spreading axes, may be the preferential sites of subduction initiation. In this model, serpentine- and talc-bearing detachment fault systems are inherently weak zones in the oceanic lithosphere that can take up ridge-perpendicular compressional stresses to nucleate subduction near and parallel to the ridge axis. Applying this detachment-induced subduction initiation model to the Jurassic Mirdita ophiolite in the northern Albanides, Maffione et al. (2015) and van Hinsbergen et al. (2015) suggested that the SSZ oceanic crust preserved in this ophiolite was produced above an east-dipping subduction zone, which was initiated along an east-dipping, near-ridge-axis detachment fault. While mechanistically this detachment-induced subduction initiation model appears feasible, its east-dipping subduction polarity does not explain the progressive melt evolution of ophiolitic magmas and their geochemical affinities in an eastward extended and propagated forearc tectonic setting, as documented in this study. It also does not provide a kinematically plausible explanation for the eastward tectonic emplacement of the Mirdita ophiolite onto the Pelagonian microcontinent prior to the Late Jurassic. Therefore, we do not consider this subduction-initiation model applicable to the tectonomagmatic evolution of the Jurassic ophiolites in the Albanides-Hellenides and their emplacement mechanisms.

Alternative models to subduction initiation at a ridge axis or along a ridge-parallel oceanic detachment fault elicit plate failure along an oceanic fracture zone or a transform fault caused by a change in relative plate motion along an active ridge-transform system (Pearce et al., 1992; Stern, 2004). Recent investigations in the IBM arc-trench system in the western Pacific (e.g., Reagan et al., 2010; Ishizuka et al., 2006; Li et al., 2013) have shown that this model of subduction initiation at an oceanic transform fault–fracture zone is realistic, and that the IBM subduction may have begun along a transform fault or fracture zone separating the old (and cold) Pacific plate from the young (and hot) Philippine Sea plate. As the old, dense Pacific lithosphere started sinking into the mantle and retreating, the displaced asthenosphere began to rise, triggering partial melting at shallow depths.

A different scenario for subduction initiation along a transform fault–fracture zone system envisions slab failure at a transform fault domain of a mid-ocean ridge spreading environment, whereby its spreading axis remains active at the leading edge of the upper plate, orthogonal to the newly formed trench (Dewey and Casey, 2011). In this model, SSZ oceanic crust generation takes place along the preexisting mid-ocean ridge axis, and the structural fabric (i.e., sheeted dike orientations, extensional normal fault attitudes) within the newly forming SSZ oceanic crust develops perpendicular to the trench axis and to the direction of tectonic emplacement of the SSZ ophiolite. Although these particular subduction-initiation dynamics may explain the structural architecture and the regional tectonics of some other ophiolites in the world (i.e., the Appalachian-Caledonian ophiolite belt in Newfoundland, Canada; Dewey and Casey, 2011), it does not apply to the Jurassic ophiolites in the Albanides-Hellenides because the documented structural fabric orientations and the emplacement kinematics of these ophiolites are incompatible with the predictions of this model.

Other alternative models for the tectonomagmatic and geodynamic evolution of the Albanide-Hellenide ophiolites have been proposed by some (see Saccani et al., 2011; Ferrière et al., 2012; Bortolotti et al., 2013, and references therein), suggesting that the Jurassic ophiolites in the Subpelagonian, Pelagonian, and Vardar zones may have formed in a single ocean located between Adria (including the Korab-Pelagonian zone, interpreted as part of the Adria domain) and Eurasia. In these models, the Mirdita-Subpelagonian-Pelagonian ophiolites are envisioned to have developed in a Middle Jurassic intraoceanic arc, evolved above

a subduction zone that was dipping north, beneath the Eurasian plate. Implicit in these models is the assumption that the present-day north-northwest–south-southeast trend of the Albanide-Hellenide belt is the result of a clockwise rotation of this belt that that took place in the latest Jurassic–Early Cretaceous (Mauritsch et al., 1996; Aiello et al., 2008; Phillips-Lander and Dilek, 2009). This scenario is reminiscent of the clockwise rotational evolution of the seafloor spreading system within the West Philippine backarc basin during the latest Eocene–Oligocene (Deschamps et al., 2002).

TECTONOMAGMATIC MODEL AND DISCUSSION

We present here a tectonomagmatic model for the evolution of the Albanide-Hellenide ophiolites (Fig. 11) that is constrained by the findings of our field-based geochemical studies and REE modeling, as well as by the recent observations and data obtained from the modern arc-trench rollback system of the IBM and its subduction initiation development.

1. The western-type N-MORBs were the first magmas to erupt after subduction initiation within the Tethyan marginal basin, and were generated as a result of decompression melting of hot, cpx-rich lithospheric mantle (Fig. 11A).

2. The initial sinking and retreat of the Tethyan slab triggered upwelling of the residual MORB mantle, with little or no mass and fluid transfer from the subducting plate. This adiabatic upwelling of the MORB-residual mantle under hot thermal conditions led to low degrees of partial melting, producing MTB melts. Contemporaneous melting of depleted MORB-type mantle resulted in the production of N-MORBs, which are now intercalated with MTBs in the WMO and Pindos volcanic sequences (Fig. 11B). The extraction of MORB and MTB melts from the peridotites in the upper plate resulted in the depletion of the mantle wedge peridotites.
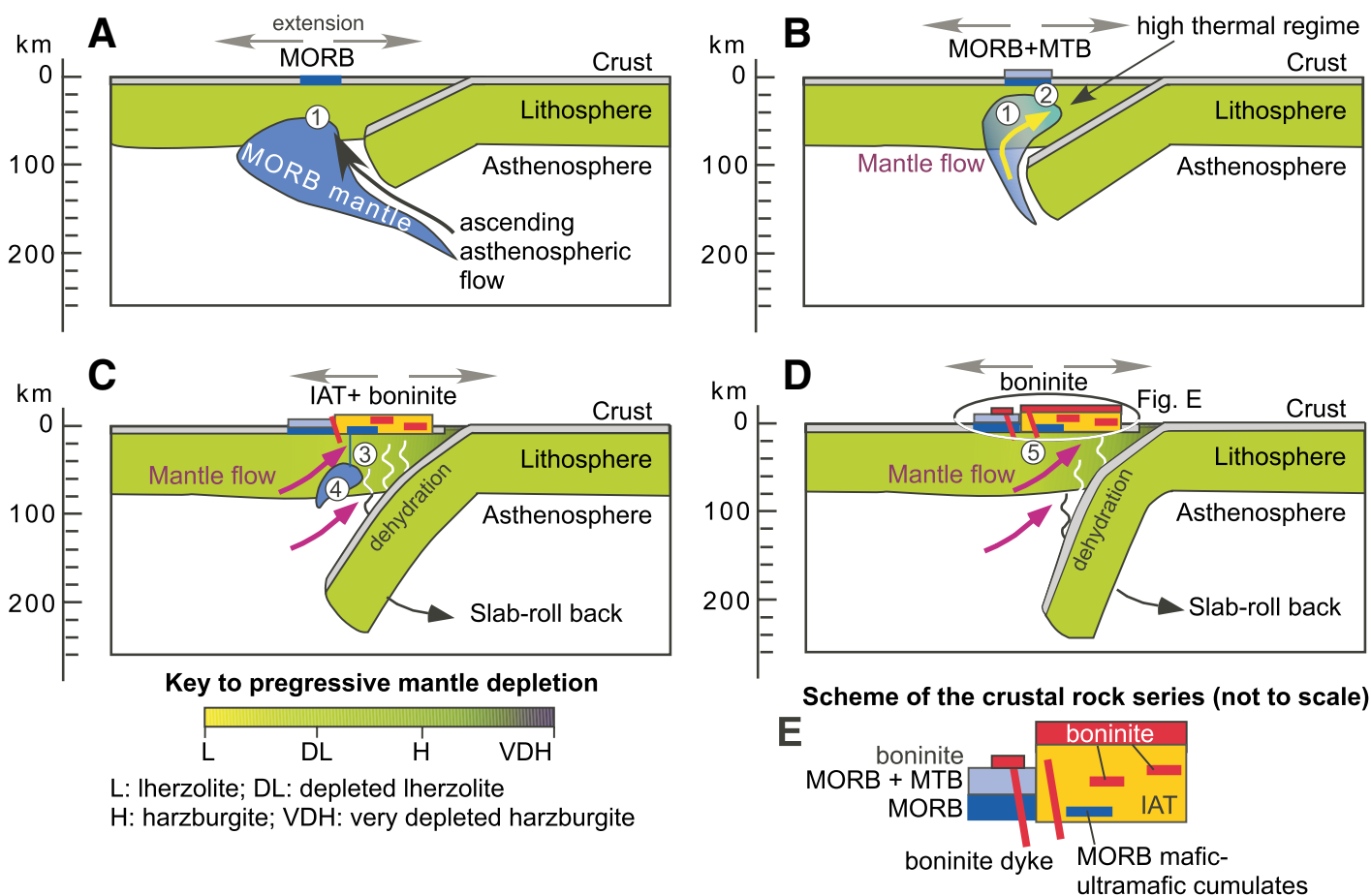
Figure 11. Two-dimensional tectonic diagrams, depicting the magmatic-petrogenetic evolution of the Jurassic ophiolites in the Albanide-Hellenide mountain belt during the subduction initiation and subduction rollback stages of a Tethyan marginal sea. Abbreviations: N-MORB—normal mid-oceanic ridge basalt, MTB—medium-Ti basalt, IAT—island arc tholeiitic basalt (low-Ti). Key to tectonomagmatic processes and upper mantle evolution (circled numbers in figures): 1—Subduction initiation. Partial melting of depleted MORB mantle produces MORBs and complementary depleted lherzolites. 2—Slab-roll back initiation. Partial melting of the residual MORB mantle produces MTBs and complementary, highly depleted lherzolites. 3—Continuing subduction and slab-rollback. Enrichment of MORB and MTB residual mantle occurs in light rare earth elements (LREEs) by subduction-derived fluids; partial melting of these refertilized sources generates IATs ± boninites, and produces harzburgites as residual mantle. 4—Waning partial melting of the depleted MORB mantle source. Very limited MORB magma production, leading to the formation of trapped mafic-ultramafic melts in the lower suprasubduction zone crust. 5—Continuing slab roll-back. Upward flow of the progressively depleted mantle toward the forearc. Continuing enrichment in LREEs of the suprasubduction depleted mantle wedge by subduction-derived fluids produces boninitic magmatism and complementary, highly depleted harzburgitic mantle.

These depleted peridotites then became the source for the later-stage IAT and boninitic magma generation.

3. Continuing slab sinking and retreat promoted accelerated return flow of the depleted mantle toward the forearc region. In the meantime, the mantle wedge peridotites were progressively enriched in fluid-mobile subduction components. These processes collectively led to the generation of IAT magmas from a depleted mantle, which was slightly enriched by subduction-derived fluids and melts. Minor volumes of boninitic magmas may have also been generated at this stage (Fig. 11C). Large volumes of boninitic magmas were produced next, when the residual depleted mantle underwent partial melting at shallow levels induced by a strong fluid flux from the subducting slab (Fig. 11D). Our melt modeling results suggest that boninite magmas were generated from high degrees of partial melting of lherzolites, or alternatively, by low degrees of partial melting of refractory harzburgites, both residual after previous multistage melt extraction events. Melting of these refractory mantle peridotites requires a high thermal regime and massive fluid flux from the subducting slab (Crawford et al., 1981, 1989; Falloon and Danyushevsky, 2000; Dilek and Furnes, 2014).

4. Diminishing MORB magmatism produced limited volumes of melts that migrated to shallow levels in the mantle wedge (Fig. 11C). These melts may have been trapped locally in the upper mantle, as evidenced by the occurrence of plagioclase peridotites in the Othrys ophiolite. These plagioclase peridotites formed as a result of refertilization of refractory harzburgites by fractionating MORB-type magmas (Barth et al., 2003, 2008). These fractionating MORB-type magmas pooled out at the upper mantle–lower crust transition and formed the MORB-type mafic-ultra-mafic cumulates (Fig. 11E) currently exposed in the eastern-type (EMO) ophiolites in the northern Albanides (Beccaluva et al., 1994; Bébien et al., 1998; Hoeck et al., 2002; Shallo and Dilek, 2003; Saccani and Tassinari, 2015).

Our field-based systematic mineralogical, geochemical, and petrogenetic modeling study of the upper mantle peridotites and extrusive sequences in the ophiolites of the Albanides-Hellenides present significant insights into the evolution of ophiolitic magmas and their mantle melt sources in a SSZ environment. A unique attribute of this study is that our classification of the upper mantle peridotite types and the subgroups of volcanic rocks in the examined ophiolites provides much needed spatial and temporal constraints for the progressive melt development in the upper plate of a subducting slab from the very early stages of subduction initiation through a mature stage of an established subduction zone. As such, this regional-scale synthesis of the magma production history of a Tethyan marginal sea oceanic lithosphere not only complements similar studies of in situ oceanic lithosphere in modern SSZ settings, but also provides a realistic petrogenetic template and a robust database for comparative studies of other well-preserved SSZ ophiolites in different orogenic belts around the world.

REFERENCES CITED

Aiello, I.W., Hagstrum, J.T., and Principi, G., 2008, Peri-equatorial paleolatitudes for Jurassic radiolarian cherts of Greece: Tectonophysics, v. 448, p. 33–48, doi:10.1016/j.tecto.2007.11.036.

Allahyari, K., Saccani, E., Pourmoafi, M., Beccaluva, L., and Masoudi, F., 2010, Petrology of mantle peridotites and intrusive mafic rocks from the Kermanshah ophiolitic complex (Zagros belt, Iran): Implications for the geodynamic evolution of the Neo-Tethyan oceanic branch between Arabia and Iran: Ofioliti, v. 35, p. 71–90.

Barth, M.G., and Gluhak, T.M., 2009, Geochemistry and tectonic setting of mafic rocks from the Othris Ophiolite, Greece: Contributions to Mineralogy and Petrology, v. 157, p. 23–40, doi:10.1007/s00410-008-0318-9.

Barth, M.G., Mason, P.R.D., Davies, G.R., Dijkstra, A.H., and Drury, M.R., 2003, Geochemistry of the Othris Ophiolite, Greece: Evidence for refertilization?: Journal of Petrology, v. 44, p. 1759–1785, doi:10.1093/petrology/egg058.

Barth, M.G., Mason, P.R.D., Davies, G.R., and Drury, M.R., 2008, The Othris ophiolite (Greece): A snapshot of subduction initiation at a mid-ocean ridge: Lithos, v. 100, p. 234–254, doi:10.1016/j.lithos.2007.06.018.

Bébien, J., Shallo, M., Manika, K., and Gega, D., 1998, The Shebenik Massif (Albania): A link between MOR- and SSZ-type ophiolites: Ofioliti, v. 23, p. 7–15.

Bébien, J., Dimo-Lahitte, A., Vergély, P., Insergueix-Filippi, D., and Dupeyrat, L., 2000, Albanian ophiolites. I—Magmatic and metamorphic processes associated with the initiation of a subduction: Ofioliti, v. 25, p. 39–45.

Beccaluva, L., and Serri, G., 1988, Boninitic and low-Ti subduction-related lavas from intra-oceanic arc-backarc systems and low-Ti ophiolites: A reappraisal of their petrogenesis and original tectonic setting: Tectonophysics, v. 146, p. 291–315, doi:10.1016/0040-1951(88)90097-2.

Beccaluva, L., Ohnenstetter, D., Ohnenstetter, M., and Paupy, A., 1984, Two magmatic series with island arc affinities within the Vourinos ophiolite: Contributions to Mineralogy and Petrology, v. 85, p. 253–271, doi:10.1007/BF00378104.

Beccaluva, L., Coltorti, M., Premti, I., Saccani, E., Siena, F., and Zeda, O., 1994, Mid-ocean ridge and suprasubduction affinities in the ophiolitic belts from Albania: Ofioliti, v. 19, p. 77–96.

Beccaluva, L., Coltorti, M., Saccani, E., and Siena, F., 2005, Magma generation and crustal accretion as evidenced by supra-subduction ophiolites of the Albanide-Hellenide Subpelagonian zone: The Island Arc, v. 14, p. 551–563, doi:10.1111/j.1440-1738.2005.00483.x.

Bloomer, S.H., Taylor, B., MacLeod, C.J., Stern, R.J., Fryer, P., Hawkins, J.W., and Johnson, L., 1995, Early arc volcanism and the ophiolite problem: A perspective from drilling in the Western Pacific, in Taylor, B., and Natland, J., eds., Active margins and marginal basins of the western Pacific: American Geophysical Union Geophysical Monograph 88, p. 1–30, doi:10.1029/GM088p0001.

Bortolotti, V., Kodra, A., Marroni, M., Mustafa, F., Pandolfi, L., Principi, G., and Saccani, E., 1996, Geology and petrology of ophiolitic sequences in the Mirdita region (northern Albania): Ofioliti, v. 21, p. 3–20.

Bortolotti, V., Marroni, M., Pandolfi, L., Principi, G., and Saccani, E., 2002, Interaction between mid-ocean ridge and subduction magmatism in Albanian ophiolites: Journal of Geology, v. 110, p. 561–576, doi:10.1086/341758.

Bortolotti, V., Marroni, M., Pandolfi, L., and Principi, G., 2005, Mesozoic to Tertiary tectonic history of the Mirdita ophiolites, northern Albania: The Island Arc, v. 14, p. 471–493, doi:10.1111/j.1440-1738.2005.00479.x.

Bortolotti, V., Chiari, M., Marroni, M., Pandolfi, L., Principi, G., and Saccani, E., 2013, The geodynamic evolution of the ophiolites from Albania and Greece, Dinaric-Hellenic belt: One, two or more oceanic basins?: International Journal of Earth Sciences, v. 102, p. 783–811, doi:10.1007/s00531-012-0835-7.

Brunelli, D., Paganelli, E., and Seyler, M., 2014, Percolation of enriched melts during incremental open-system melting in the spinel field: A REE approach to abyssal peridotites from the Southwest Indian Ridge: Geochimica et Cosmochimica Acta, v. 127, p. 190–203, doi:10.1016/j.gca.2013.11.040.

Capedri, S., Venturelli, G., and Toscani, L., 1982, Petrology of an ophiolitic cumulate sequence from Pindos, Greece: Geological Journal, v. 17, p. 223–242, doi:10.1002/gj.3350170304.

Capedri, S., Lekkas, E., Papanicolaou, D., Skarpelis, N., Venturelli, G., and Gallo, F., 1985, The ophiolite of the Koziakas range western Thessaly (Greece): Neues Jahrbuch für Mineralogie, Abhandlungen, v. 152, p. 45–64.

Chiari, M., Marcucci, M., and Prela, M., 2002, New species of Jurassic radiolarian in the sedimentary cover of ophiolites in the Mirdita area, Albania: Micropaleontology, v. 48, p. 61–87.

Chiari, M., Bortolotti, V., Marcucci, M., Photiades, A., and Principi, G., 2003, The middle Jurassic siliceous sedimentary cover at the top of the Vourinos ophiolite (Greece): Ofioliti, v. 28, p. 95–103.

Chiari, M., Marcucci, M., and Prela, M., 2004, Radiolarian assemblages from the Jurassic cherts of Albania: New data: Ofioliti, v. 29, p. 95–105.

Crawford, A.J., Beccaluva, L., and Serri, G., 1981, Tectono-magmatic evolution of the West Philippine–Mariana region and the origin of boninites: Earth and Planetary Science Letters, v. 54, p. 346–356, doi:10.1016/0012-821X(81)90016-9.

Crawford, A.J., Falloon, A., and Green, D.H., 1989, Classification, petrogenesis and tectonic setting of boninites, in Crawford, A.J., ed., Boninites and related rocks: London, Unwin Hyman, p. 1–49.

Dede, S., Shehu, R., and Shallo, M., 1966, Le magnetisme intrusive et ses mineralisations en Albanie: Permbledhje Studimesh, v. 3, p. 3–35 (in Albanian with a French summary).

Deschamps, A., Kanatoro, F., and Kyoko, O., 2002, Late amagmatic extension along the central and eastern segments of the West Philippine Basin fossil spreading axis: Earth and Planetary Science Letters, v. 203, p. 277–293, doi:10.1016/S0012-821X(02)00855-5.

Dewey, J.F., and Casey, J.F., 2011, The origin of obducted large-slab ophiolite complexes, in Brown, D., and Ryan, P., eds., Arc-continent collision: The making of an orogen: Frontiers in Earth Sciences: Heidelberg, Springer, p. 431–444, doi:10.1007/978-3-540-88558-0_15.

Dilek, Y., 2003, Ophiolites pulses, mantle plumes and orogeny, in Dilek, Y., and Robinson, P.T., eds., Ophiolites in Earth history: Geological Society of London Special Publication 218, p. 9–19, doi:10.1144/GSL.SP.2003.218.01.02.

Dilek, Y., 2006, Collision tectonics of the Eastern Mediterranean region: Causes and consequences, in Dilek, Y., and Pavlides, S., eds., Postcollisional tectonics and magmatism in the Mediterranean region and Asia: Geological Society of America Special Paper 409, p. 1–13, doi:10.1130/2006.2409(1).

Dilek, Y., and Flower, M.F.J., 2003, Arc-trench rollback and forearc accretion: 2. A model template for ophiolites in Albania, Cyprus, and Oman, in Dilek, Y., and Robinson, P.T., eds., Ophiolites in Earth history: Geological Society of London Special Publication 218, p. 43–68, doi:10.1144/GSL.SP.2003.218.01.04.

Dilek, Y., and Furnes, H., 2009, Structure and geochemistry of Tethyan ophiolites and their petrogenesis in subduction rollback systems: Lithos, v. 113, p. 1–20, doi:10.1016/j.lithos.2009.04.022.

Dilek, Y., and Furnes, H., 2011, Ophiolite genesis and global tectonics: Geochemical and tectonic fingerprinting of ancient oceanic lithosphere: Geological Society of America Bulletin, v. 123, p. 387–411, doi:10.1130/B30446.1.

Dilek, Y., and Furnes, H., 2014, Ophiolites and their origins: Elements, v. 10, p. 93–100, doi: 10.2113/gselements.10.2.93.

Dilek, Y., and Newcomb, S., eds., 2003, Ophiolite concept and the evolution of geological thought: Geological Society of America Special Paper 373, 504 p., doi:10.1130/SPE373.

Dilek, Y., and Robinson, P.T., 2003, Introduction, in Dilek, Y., and Robinson, P.T., eds., Ophiolites in Earth history: Geological Society of London Special Publication 218, p. 1–8, doi: 10.1144/GSL.SP.2003.218.01.01.

Dilek, Y., and Thy, P., 1998, Structure, petrology, and seafloor spreading tectonics of the Kizildag ophiolite (Turkey), in Mills, R., and Harrison, K., eds., Modern ocean floor processes and the geological record: Geological Society of London Special Publication 148, p. 43–69, doi:10.1144/GSL.SP.1998.148.01.04.

Dilek, Y., and Thy, P., 2009, Island arc tholeiite to boninitic melt evolution of the Cretaceous Kizildag (Turkey) ophiolite: Model for multi-stage early arc-forearc magmatism in Tethyan subduction factories: Lithos, v. 113, p. 68–87, doi:10.1016/j.lithos.2009.05.044.

Dilek, Y., Shallo, M., and Furnes, H., 2005, Rift-drift, seafloor spreading, and subduction tectonics of Albanian ophiolites: International Geology Review, v. 47, p. 147–176, doi:10.2747/0020-6814.47.2.147.

Dilek, Y., Furnes, H., and Shallo, M., 2007, Suprasubduction zone ophiolite formation along the periphery of Mesozoic Gondwana: Gondwana Research, v. 11, p. 453–475, doi:10.1016/j.gr.2007.01.005.

Dilek, Y., Furnes, H., and Shallo, M., 2008, Geochemistry of the Jurassic Mirdita Ophiolite (Albania) and the MORB to SSZ evolution of a marginal basin oceanic crust: Lithos, v. 100, p. 174–209, doi:10.1016/j.lithos.2007.06.026.

Dijkstra, A.H., Barth, M.G., Drury, M.R., Mason, P.R.D., and Vissers, R.L.M., 2003, Diffuse porous melt flow and melt-rock reaction in the mantle lithosphere at a slow-spreading ridge: A structural petrology and LA-ICP-MS study of the Othris Peridotite Massif (Greece): Geochemistry, Geophysics, Geosystems, v. 4, 8613, doi:10.1029/2001GC000278.

Dobson, P.F., Blank, J.G., Maruyama, S., and Liu, G., 2006, Petrology and geochemistry of boninite series volcanic rocks, Chichi-jima, Bonin Islands, Japan: International Geology Review, v. 48, p. 669–701, doi:10.2747/0020-6814.48.8.669.

Elliott, T., and Spiegelman, M., 2003, Melt migration in oceanic crustal production: A U-series perspective, in Rudnick, R.L., ed., Treatise on geochemistry Volume 3: Amsterdam, Elsevier, p. 465–510, doi:10.1016/B0-08-043751-6/03031-0.

Falloon, T.J., and Danyushevsky, L.V., 2000, Melting of refractory mantle at 1.5, 2 and 2.5 GPa under anhydrous and H₂O-undersaturated conditions: Implications for the petrogenesis of high-Ca boninites and the influence of subduction components on mantle melting: Journal of Petrology, v. 41, p. 257–283, doi:10.1093/petrology/41.2.257.

Ferrière, J., Chanier, F., and Ditbanjong, P., 2012, The Hellenic ophiolites: Eastward or westward obduction of the Maliac Ocean, a discussion: International Journal of Earth Sciences, v. 101, p. 1559–1580, doi:10.1007/s00531-012-0797-9.

Flower, M.F.J., and Dilek, Y., 2003, Arc-trench rollback and forearc accretion: 1. A collision-induced mantle flow model for Tethyan ophiolites, in Dilek, Y., and Robinson, P.T., eds., Ophiolites in Earth history: Geological Society of London Special Publication 218, p. 21–41, doi:10.1144/GSL.SP.2003.218.01.03.

Gribble, R.F., Stern, R.J., Bloomer, S.H., Stuben, D., O'Hearn, T., and Newman, S., 1996, MORB mantle and subduction components interact to generate basalts in the southern Mariana Trough back-arc basin: Geochimica et Cosmochimica Acta, v. 60, p. 2153–2166, doi: 10.1016/0016-7037(96)00078-6.

Hart, S.R., and Zindler, A., 1986, In search of the bulk Earth composition: Chemical Geology, v. 57, p. 247–267, doi:10.1016/0009-2541(86)90053-7.

Hoeck, V., Koller, F., Meisel, T., Onuzi, K., and Kneringer, E., 2002, The Jurassic South Albanian ophiolites: MOR- vs. SSZ-type ophiolites: Lithos, v. 65, p. 143–164, doi:10.1016/S0024-4937(02)00163-9.

Insergueix-Filippi, D., Dupeyrat, L., Dimo, A., Vergély, P., and Bébien, J., 2000, Albanian ophiolites: II—Model of subduction zone infancy at a mid-ocean ridge: Ofioliti, v. 25, p. 47–53.

Ishizuka, O., et al., 2006, Early stages in the evolution of Izu-Bonin arc volcanism: New age, chemical, and isotopic constraints: Earth and Planetary Science Letters, v. 250, p. 385–401, doi:10.1016/j.epsl.2006.08.007.

Jagoutz, E., Palme, H., Baddenhausen, H., Blum, K., Candales, M., Dreibus, C., Spettel, B., Lorenz, V., and Wanke, H., 1979, The abundances of major and trace elements in the Earth's mantle as derived from primitive ultramafic nodules: Lunar and Planetary Science Conference, 10th, Proceedings, v. 2, p. 2031–2050.

Jones, G., and Robertson, A.H.F., 1991, Tectono-stratigraphy and evolution of the Pindos ophiolite and related units, northwestern Greece: Journal of the Geological Society [London], v. 148, p. 267–288, doi:10.1144/gsjgs.148.2.0267.

Kelemen, P.B., Shimizu, N., and Salters, V.J.M., 1995, Extraction of mid-ocean-ridge basalt from the upwelling mantle by focused flow of melt in dunite channels: Nature, v. 375, p. 747–753, doi:10.1038/375747a0.

Koller, F., Hoeck, V., Meisel, T., Ionescu, C., Onuzi, K., and Ghega, D., 2006, Cumulates and gabbros in southern Albanian ophiolites: Their bearing on regional tectonic setting, in Robertson, A.H.F., and Mountrakis, D., eds., Tectonic development of the eastern Mediterranean region: Geological Society of London Special Publication 260, p. 267–299, doi: 10.1144/GSL.SP.2006.260.01.12.

Kostopoulos, D.K., and Murton, B.J., 1992, Origin and distribution of components in boninite genesis: Significance of the OIB component, in Parson, L.M., et al., eds., Ophiolites and their modern oceanic analogues: Geological Society of London Special Publication 60, p. 133–154, doi:10.1144/GSL.SP.1992.060.01.08.

Lachance, G.R., and Trail, R.J., 1966, Practical solution to the matrix problem in X-ray analysis: Canadian Spectroscopy, v. 11, p. 43–48.

Lambart, S., Laporte, D., Provost, A., and Schiano, P., 2012, Fate of pyroxenite-derived melts in the peridotitic mantle: Thermodynamic and experimental constraints: Journal of Petrology, v. 53, p. 451–476, doi:10.1093/petrology/egr068.

Li, Y.-B., et al., 2013, High-Mg adakite and low-Ca boninite from a Bonin fore-arc seamount: Implications for the reaction between slab melts and depleted mantle: Journal of Petrology, v. 54, p. 1149–1175, doi:10.1093/petrology/egt008.

Macdonald, R., Hawkesworth, C.J., and Heath, E., 2000, The Lesser Antilles volcanic chain: A study in arc magmatism: Earth-Science Reviews, v. 49, p. 1–76, doi:10.1016/S0012-8252(99)00069-0.

Maffione, M., Thieulot, C., van Hinsbergen, D.J.J., Morris, A., Plümper, O., and Spakman, W., 2015, Dynamics of intraoceanic subduction initiation: 1. Oceanic detachment fault inversion and the formation of supra-subduction zone ophiolites: Geochemistry, Geophysics, Geosystems, v. 16, p. 1753–1770, doi:10.1002/2015GC005746.

Manika, K., Shallo, M., Bébien, J., and Gega, D., 1997, The plutonic sequence of Shebenik ophiolite complex, Albania: Evidence for dual magmatism: Ofioliti, v. 22, p. 93–99.

Marcucci, M., and Prela, M., 1996, The Lumi i zi (Puke) section of the Kalur Cherts: Radiolarian assemblages and comparison with other sections in northern Albania: Ofioliti, v. 21, p. 71–76.

Mauritsch, H.J., Sholger, R., Bushati, S.L., and Xhomo, A., 1996, Palaeomagnetic investigations in northern Albania and their significance for the geodynamic evolution of the Adriatic-Aegean realm, in Morris, A., and Tarling, D.H., eds., Paleomagnetism and tectonics of the Mediterranean region: Geological Society of London Special Publication 105, p. 265–275, doi:10.1144/GSL.SP.1996.105.01.23.

Mercier, J.-C.C., and Nicolas, A., 1975, Textures and fabrics of upper mantle peridotites as illustrated by xenoliths from basalts: Journal of Petrology, v. 16, p. 454–487, doi:10.1093/petrology/16.2.454.

Monjoie, P., Lapierre, H., Tashko, A., Mascle, G.H., Dechamp, A., Muceku, B., and Brunet, P., 2008, Nature and origin of the Triassic volcanism in Albania and Othrys: A key to understanding the Neotethys opening?: Bulletin de la Société Géologique de France, v. 179, p. 411–425, doi:10.2113/gssgfbull.179.4.411.

Morishita, T., Dilek, Y., Shallo, M., Tamura, A., and Arai, S., 2011, Insight into the uppermost mantle section of a maturing arc: The Eastern Mirdita ophiolite, Albania: Lithos, v. 124, p. 215–226, doi:10.1016/j.lithos.2010.10.003.

Murton, B.J., 1989, Tectonic controls on boninite genesis, in Saunders, A.D.N., and Norry, M.J., eds., Magmatism in the ocean basins: Geological Society of London Special Publication 42, p. 347–377, doi:10.1144/GSL.SP.1989.042.01.20.

Niu, Y., 1997, Mantle melting and melt extraction processes beneath ocean ridges: Evidence from abyssal peridotites: Journal of Petrology, v. 38, p. 1047–1074, doi:10.1093/petroj/38.8.1047.

Parkinson, I.J., and Pearce, J.A., 1998, Peridotites from the Izu-Bonin-Mariana forearc (ODP Leg 125): Evidence for mantle melting and melt-mantle interaction in a suprasubduction zone setting: Journal of Petrology, v. 39, p. 1577–1618, doi:10.1093/petroj/39.9.1577.

Pearce, J.A., 1982, Trace element characteristics of lavas from destructive plate boundaries, in Thorpe, R.S., ed., Andesites: New York, Wiley, p. 525–548.

Pearce, J.A., 2008, Geochemical fingerprinting of oceanic basalts with applications to ophiolite classification and the search for Archean oceanic crust: Lithos, v. 100, p. 14–48, doi: 10.1016/j.lithos.2007.06.016.

Pearce, J.A., and Norry, M.J., 1979, Petrogenetic implications of Ti, Zr, Y, and Nb variations in volcanic rocks: Contributions to Mineralogy and Petrology, v. 69, p. 33–47, doi:10.1007/BF00375192.

Pearce, J.A., and Parkinson, I.J., 1993, Trace element models for mantle melting: Application to volcanic arc petrogenesis, in Prichard, H.M., et al., eds., Magmatic processes and plate tectonics: Geological Society of London Special Publication 76, p. 373–403, doi:10.1144/GSL.SP.1993.076.01.19.

Pearce, J.A., and Peate, D.W., 1995, Tectonic implications of the composition of volcanic arc magmas: Annual Review of Earth and Planetary Sciences, v. 23, p. 251–285, doi:10.1146/annurev.ea.23.050195.001343.

Pearce, J.A., van der Laan, S.R., Arculus, R.J., Murton, B.J., Ishii, T., Peate, D.W., and Parkinson, I.J., 1992, Boninite and harzburgite from Leg 125 (Bonin-Mariana forearc): A case study of magma genesis during the initial stage of subduction, in Fryer P., et al., eds., Proceedings of the Ocean Drilling Program, Scientific Results, Volume 125: College Station, Texas, Ocean Drilling Program, p. 623–659, doi:10.2973/odp.proc.sr.125.172.1992.

Phillips-Lander, C., and Dilek, Y., 2009, Structural architecture of the sheeted dike complex and extensional tectonics of the Jurassic suprasubduction zone Mirdita ophiolite, Albania: Lithos, v. 108, p. 192–206, doi:10.1016/j.lithos.2008.09.014.

Photiades, A., Saccani, E., and Tassinari, R., 2003, Petrogenesis and tectonic setting of volcanic rocks from the Subpelagonian ophiolitic mélange in the Agoriani area (Othrys, Greece): Ofioliti, v. 28, p. 121–135.

Rassios, A.E., and Dilek, Y., 2009, Rotational deformation in the Jurassic Mesohellenic ophiolites, Greece, and its tectonic significance: Lithos, v. 108, p. 207–223, doi:10.1016/j.lithos .2008.09.005.

Reagan, M.K., et al., 2010, Fore-arc basalts and subduction initiation in the Izu-Bonin-Mariana system: Geochemistry, Geophysics, Geosystems, v. 11, Q03X12, doi:10.1029 /2009GC002871.

Saccani, E., 2015, A new method of discriminating different types of post-Archean ophiolitic basalts and their tectonic significance using Th-Nb and Ce-Dy-Yb systematics: Geoscience Frontiers, v. 6, p. 481–501, doi:10.1016/j.gsf.2014.03.006.

Saccani, E., and Photiades, A., 2004, Mid-ocean ridge and supra-subduction affinities in the Pindos Massif ophiolites (Greece): Implications for magma genesis in a proto-forearc setting: Lithos, v. 73, p. 229–253, doi:10.1016/j.lithos.2003.12.002.

Saccani, E., and Photiades, A., 2005, Petrogenesis and tectono-magmatic significance of volcanic and subvolcanic rocks in the Albanide-Hellenide ophiolitic mélanges: The Island Arc, v. 14, p. 494–516, doi:10.1111/j.1440-1738.2005.00480.x.

Saccani, E., and Tassinari, R., 2015, The role of MORB and SSZ magma-types in the formation of Jurassic ultramafic cumulates in the Mirdita ophiolites (Albania) as deduced from chromian spinel and olivine chemistry: Ofioliti, v. 40, p. 37–56, doi:10.4454/ofioliti.v40i1.434.

Saccani, E., Photiades, A., and Padoa, E., 2003, Geochemistry, petrogenesis and tectono-magmatic significance of volcanic and subvolcanic rocks from the Koziakas Mélange (western Thessaly, Greece): Ofioliti, v. 28, p. 43–57.

Saccani, E., Beccaluva, L., Coltorti, M., and Siena, F., 2004, Petrogenesis and tectono-magmatic significance of the Albanide-Hellenide ophiolites: Ofioliti, v. 29, p. 77–95.

Saccani, E., Photiades, A., Santato, A., and Zeda, O., 2008a, New evidence for supra-subduction zone ophiolites in the Vardar zone from the Vermion massif (northern Greece): Implication for the tectono-magmatic evolution of the Vardar oceanic basin: Ofioliti, v. 33, p. 17–37.

Saccani, E., Photiades, A., and Beccaluva, L., 2008b, Petrogenesis and tectonic significance of IAT magma-types in the Hellenide ophiolites as deduced from the Rhodiani ophiolites (Pelagonian zone, Greece): Lithos, v. 104, p. 71–84, doi:10.1016/j.lithos.2007.11.006.

Saccani, E., Beccaluva, L., Photiades, A., and Zeda, O., 2011, Petrogenesis and tectono-magmatic significance of basalts and mantle peridotites from the Albanian-Greek ophiolites and sub-ophiolitic mélanges. New constraints for the Triassic–Jurassic evolution of the Neo-Tethys in the Dinaride sector: Lithos, v. 124, p. 227–242, doi:10.1016/j.lithos.2010 .10.009.

Salters, V.J.M., and Stracke, A., 2004, Composition of the depleted mantle: Geochemistry, Geophysics, Geosystems, v. 5, Q05004, doi:10.1029/2003GC000597.

Shallo, M., 1992, Geological evolution of the Albanian ophiolite and their platform periphery: Geologische Rundschau, v. 81, p. 681–694, doi:10.1007/BF01791385.

Shallo, M., 1994, Outline of the Albanian ophiolites: Ofioliti, v. 19, p. 57–75.

Shallo, M., and Dilek, Y., 2003, Development of the ideas on the origin of Albanian ophiolites, in Dilek, Y., and Newcomb, S., eds., Ophiolite concept and the evolution of geological thought: Geological Society of America Special Paper 373, p. 351–363, doi:10.1130 /0-8137-2373-6.351.

Shallo, M., Kote, D., and Vranaj, A., 1987, Geochemistry of the volcanics from ophiolitic belts of Albanides: Ofioliti, v. 12, p. 125–136.

Shervais, J.W., 1982, Ti-V plots and the petrogenesis of modern ophiolitic lavas: Earth and Planetary Science Letters, v. 59, p. 101–118, doi:10.1016/0012-821X(82)90120-0.

Smith, A.G., 1993, Tectonic significance of the Hellenic-Dinaric ophiolites, in Princiard, H.M., et al., eds., Magmatic processes and plate tectonics: Geological Society of London Special Publication 76, p. 213–243, doi:10.1144/GSL.SP.1993.076.01.10.

Stern, R.J., 2004, Subduction initiation: Spontaneous and induced: Earth and Planetary Science Letters, v. 226, p. 275–292, doi:10.1016/S0012-821X(04)00498-4.

Stern, R.J., Fouch, M.J., and Klemperer, S., 2003, An overview of the Izu-Bonin-Mariana subduction factory, in Eiler, J.M., ed., Inside the subduction factory: American Geophysical Union Geophysical Monograph 138, p. 175–222, doi:10.1029/138GM10.

Sun, S.S., and McDonough, W.F., 1989, Chemical and isotopic systematics of ocean basalts: Implications for mantle composition and processes, in Saunders, A.D., and Norry, M.J., eds., Magmatism in the ocean basins: Geological Society of London Special Publication 42, p. 313–346, doi:10.1144/GSL.SP.1989.042.01.19.

Takazawa, E., Frey, F.A., Shimizu, N., Obata, M., and Bodinier, J.L., 1992, Geochemical evidence for melt migration and reaction in the upper mantle: Nature, v. 359, p. 55–58, doi: 10.1038/359055a0.

Taylor, B., and Martinez, F., 2003, Back-arc basin basalt systematics: Earth and Planetary Science Letters, v. 210, p. 481–497, doi:10.1016/S0012-821X(03)00167-5.

Uysal, I., Ersoy, E.Y., Karsli, O., Dilek, Y., Sadiklar, M.B., Ottley, C.J., Tiepolo, M., and Meisel, T., 2012, Coexistence of abyssal and ultra-depleted SSZ type mantle peridotites in a Neo-Tethys ophiolite in SW Turkey: Constraints from mineral composition, whole-rock geochemistry (major- trace-REE-PGE), and Re-Os isotope systematics: Lithos, v. 132–133, p. 50–69, doi:10.1016/j.lithos.2011.11.009.

Van der Laan, S.R., Arculus, R.L., Pearce, J.A., and Murton, B.J., 1992, Petrography, mineral chemistry and phase relations of the basement boninite series of Site 786, Izu-Bonin forearc, in Fryer, P., et al., eds., Proceedings of the Ocean Drilling Program, Scientific Results, Volume 125: College Station, Texas, Ocean Drilling Program, p. 171–201, doi:10 .2973/odp.proc.sr.125.139.1992.

van Hinsbergen, D.J.J., et al., 2015, Dynamics of intraoceanic subduction initiation: 2. Suprasubduction zone ophiolite formation and metamorphic sole exhumation in context of absolute plate motions: Geochemistry, Geophysics, Geosystems, v. 16, p. 1771–1785, doi:10.1002/2015GC005745.

Warren, J.M., 2016, Global variations in abyssal peridotite compositions: Lithos, v. 248–251, p. 193–219, doi:10.1016/j.lithos.2015.12.023.

Workman, R.K., and Hart, S.R., 2005, Major and trace element composition of the depleted MORB mantle (DMM): Earth and Planetary Science Letters, v. 231, p. 53–72, doi:10.1016 /j.epsl.2004.12.005.

Wu, W.W., Yang, J.S., Dilek, Y., Milushi, I., and Lian, D.Y., 2017, Multiple episodes of melting, depletion, and enrichment of the Tethyan mantle: Petrogenesis of the peridotites and chromitites in the Jurassic Skenderbeu massif, Mirdita ophiolite, Albania: Lithosphere, doi:10.1130/L606.1.

Yuan, C., Sun, M., Zhou, M.-F., Xiao, W., and Zhou, H., 2005, Geochemistry and petrogenesis of the Yishak Volcanic Sequence, Kudi ophiolite, West Kunlun (NW China): Implications for the magmatic evolution in a subduction zone environment: Contributions to Mineralogy and Petrology, v. 150, p. 195–211, doi:10.1007/s00410-005-0012-0.